Application of bio-based electrodes in emerging capacitive deionization technology for desalination and wastewater treatment

Sayed, Enas Taha; Olabi, A.G.; Shehata, Nabila; Al Radi, Muaz; Majdy Muhaisen, Omar; Rodriguez, Cristina; Ali Atieh, Muataz; Abdelkareem, Mohammad Ali

Published in:
Ain Shams Engineering Journal

DOI:
10.1016/j.asej.2022.102030

E-pub ahead of print: 28/10/2022

Document Version
Publisher's PDF, also known as Version of record

Ain Shams Engineering Journal xxx (xxxx) xxx

Contents lists available at ScienceDirect

Ain Shams Engineering Journal

journal homepage: www.sciencedirect.com

Application of bio-based electrodes in emerging capacitive deionization technology for desalination and wastewater treatment

Enas Taha Sayed [a,b], A.G. Olabi [c,d,*], Nabila Shehata [e], Muaz Al Radi [f], Omar Majdy Muhaisen [c], Cristina Rodriguez [g], Muataz Ali Atieh [a,h,*], Mohammad Ali Abdelkareem [a,b,c,*]

[a] Center for Advanced Materials Research, University of Sharjah, P.O. Box 27272, Sharjah, United Arab Emirates
[b] Chemical Engineering Department, Minia University, Elminia, Egypt
[c] Sustainable Energy & Power Systems Research Centre, RISE, University of Sharjah, P.O. Box 27272, Sharjah, United Arab Emirates
[d] Mechanical Engineering and Design, Aston University, School of Engineering and Applied Science, Aston Triangle, Birmingham B4 7ET, UK
[e] Department of Environmental Science and Industrial Development Department, Faculty of Postgraduate Studies for Advanced Sciences, Beni-Suef University, Beni-Suef, Egypt
[f] Department of Electrical Engineering and Computer Science, Khalifa University, Abu Dhabi, United Arab Emirates
[g] School of Computing, Engineering and Physical Sciences, University of the West of Scotland, Paisley PA1 2BE, UK
[h] Department of Mechanical and Nuclear Engineering, University of Sharjah, 27272 Sharjah, United Arab Emirates

ARTICLE INFO

Article history:
Received 6 July 2022
Revised 2 October 2022
Accepted 16 October 2022
Available online xxxx

Keywords:
Capacitive deionization (CDI)
Bio-based electrodes
Water desalination
Wastewater treatment

ABSTRACT

Capacitive deionization (CDI) is an emerging, efficient, cheap, and environmentally friendly water desalination technology. One of the most critical components of the CDI system is the electrodes; thus, improving their performance will promote its commercial application. The cost, efficiency, and availability of the electrode materials are the main challenges facing the application of the CDI in water desalination and wastewater treatment compared to other technologies. To reduce the cost of the electrodes, carbon materials derived from biomass and general wastes are being considered. A detailed review of the application of bio-based derived electrodes in CDI desalination and wastewater treatment is presented. A comparison between these novel materials and conventional carbon nanomaterials is discussed in terms of resource availability, ease of manufacture, cost, material specifications, and performance. Finally, future research recommendations are introduced to enhance this technology's feasibility and performance.

1. Introduction

Water covers 70 % of the planet's surface, but only 1 % is a freshwater source [1]. Rapid human population growth and technological advances resulted in clean drinking water scarcity. Meanwhile, wastewater is generated daily in huge quantities and requires enormous amounts of energy for proper treatment before safe discharge [2–5]. Several methods have been introduced for water purification and recovery from wastewater besides water desalination technologies [6]. These technologies are based on thermal separation, selective membrane permeabilities, chemical potential differences, or electrical charge separation. Although membrane-based separation is economically feasible compared to thermal-based methods, it still requires a considerable portion of energy from fossil fuels with high environmental impacts [7].

Emerging technologies such as forward osmosis (FO) [8], capacitive deionization (CDI) [9–11], electrodialysis (ED) [12,13], electrodialysis reversal (EDR) [14], and microbial desalination cells (MDC) [15,16], have lower energy consumption and lower environmental impacts than traditional methods [17,18]. Among these methods, Capacitive deionization (CDI) is the most attractive because it has high energy efficiency, no need for high-pressure pumps, environmentally friendly, simple in operation, and lower energy consumption [19–21]. Moreover, it can be integrated into

* Corresponding authors at: Mechanical Engineering and Design, Aston University, School of Engineering and Applied Science, Aston Triangle, Birmingham B4 7ET, UK (A.G. Olabi) and Center for Advanced Materials Research, University of Sharjah, P.O. Box 27272, Sharjah, United Arab Emirates (Muataz Ali Atieh and Mohammad Ali Abdelkareem).
E-mail addresses: aolabi@sharjah.ac.ae (A.G. Olabi), mhussien@sharjah.ac.ae (M. Ali Atieh), mabdulkareem@sharjah.ac.ae (M.A. Abdelkareem).

Peer review under responsibility of Ain Shams University.

Production and hosting by Elsevier

https://doi.org/10.1016/j.asej.2022.102030
2090-4479/

solar energy or any other renewable energy source in isolated regions with no or low environmental impacts [22].

A CDI unit consists of two porous electrodes (often carbon electrodes) and a separator (either a porous dielectric material or an open channel) inserted between them. The electrodes are subjected to a potential difference (typically 1–1.4 V) [23]. The saline or contaminated water passes between the positive and negative electrodes, where the unwanted ions in the water move into an electric double layer (EDL) along the electrode-water interface, thus eliminating the unwanted salts or contaminants [24] in an electrosorption process on the electrode surfaces (Fig. 1(a)). The ions are electrostatically held in the electrode surface and released with reversing polarity in the discharging stage "desorption process" [25] (Fig. 1(b)). A CDI unit can complete thousands of adsorption–desorption cycles. The degradation of the electrodes will lead to a reduced cell's lifetime. Oxygen and some organic compounds [26] present in the water can degrade electrodes by oxidation [27], reducing the electrosorption capacity and the cell's lifetime [28].

Porous carbon electrodes have a high surface area, are stable at a wide temperature and pH windows, and have excellent adsorption capabilities; therefore, they were extensively applied in the CDI'electrodes [29–34]. Bio-based carbon materials are cheap with no environmental impact; therefore, they are an excellent candidate to replace activated carbon. These bio-based carbon materials demonstrated promising results in several applications, such as supercapacitors [35–38], fuel cells [39–42], batteries [43,44], and CDI [45–49].

The CDI performance depends on the electrode's materials; thus, proper material selection is important for achieving high cell performance. The electrode materials must have salt electrosorption capacity, high specific capacity, and sufficient strength to maintain the cell's hydrodynamic forces during cell operation. The materials must also have good biofouling resistance, high absorptivity, i.e., hydrophilic, and high capability [50,51]. Furthermore, they must be free from chemicals that harm humans, animals, or ecosystems [52]. Traditional carbon materials used in electrodes include carbon nanotubes, carbon nanofibers, carbon aerogels, activated carbon, and graphene. These materials are produced from non-renewable materials through high energy-consuming processes, which challenge large-scale production and industrial applications. Activated carbon (AC) extracted from biomass [53,54] is suitable for CDI electrode material due to its low price, availability, sustainability, and negligible environmental effect. Moreover, AC derived from biomass shows a high SSA "specific surface area", high conductivity, and well distribution of pores [55]. Therefore, it is necessary to investigate different biomass and waste resources and evaluate their suitability as a carbon source for electrode manufacturing to produce a cheap and reliable CDI system.

Several reports summarized the progress done in applying the CDI as an effective tool in water desalination [56–58], wastewater treatment, brine treatment of the RO unit [59], carbon-based materials [58,60], and the different methods for improving the performance of the carbon-based materials in the CDI system [19]. Recently Elisadiki et al. summarized the application of bio-based electrodes in the CDI for water desalination [21]. The application of bio-based carbon materials in the CDI electrode for wastewater treatment has not been made yet. Recently, many of the desalination CDI cells' biobased electrodes have been done and need to be summarized. The present work aims to critically review the recent advances in bio-based electrodes for CDI applications in water desalination and wastewater treatment. The preparation of CDI electrodes from biomass/waste resources is briefly described alongside a detailed comparison between bio-based and conventional electrodes. Finally, the current challenges for the industrial application of such electrode materials and future research recommendations are introduced.

2. Preparation methods of activated carbon from different biomass resources

Biomass is classified as living or dead organisms and all by-products of these organisms, animals or plants. Elemental analysis shows that biomass is abundant in carbon, hydrogen, oxygen, and nitrogen [61]. The main advantages of carbon derived from biomass sources are their abundance and availability, low cost, in situ nano-porous structure development, flexibility in manufacturing, and its intrinsically renewable nature [62]. Due to their high SSA "specific surface area" and excellent conductivity, biomass-derived porous carbons such as those obtained from rice husk, bacterial cellulose, or sugarcane demonstrated promising results as electrodes of the CDI cell and other applications [63]. A prober preparation method of activated carbon from biomass involves carbonization through hydrothermal and/or pyrolysis and activation to increase the surface area. The common methods for preparation and activation of biobased materials are summarized as follows:

2.1. Hydrothermal carbonization

HTC "Hydrothermal carbonization", is a thermochemical method in which the organic content is turned into nanostructured porous carbons through fractionation of the biomass feedstock [64,65]. HTC can treat wet biomass at moderately low temperatures (180–250 °C) without a pre-drying step, resulting in low production costs [66]. The process's residence time and temperature determine the severity of the reaction and biomass coalification level. The solid residue from the HTC process, known as hydrochar [67], exhibits high hydrophobic and friable properties and is easily

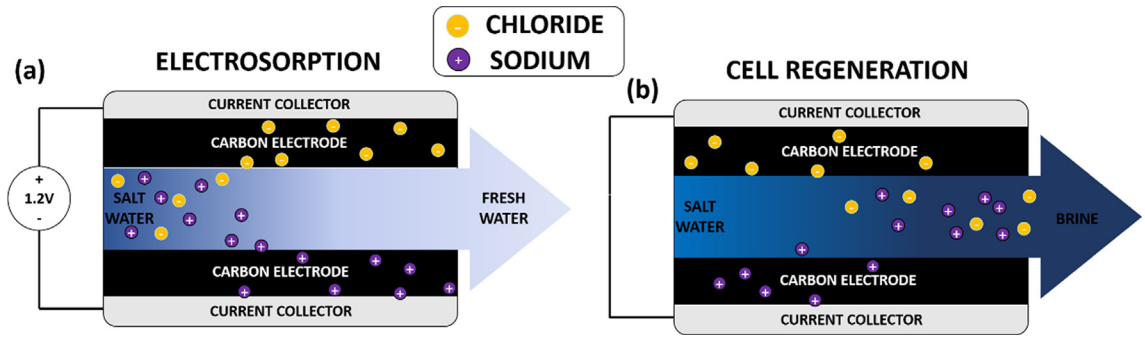

Fig. 1. CDI cell under (a) electrosorption and (b) regeneration steps.

separated from the liquid product. The hydrochar shows higher mass and energy density, improved dewaterability, and better combustion performance than raw biomass [68]. However, the hydrochar properties depend on the biomass source [69]. The hydrochar possesses a low specific surface area and poor porous nature; thus, a subsequent activation or carbonization process is necessary to modify its physical and chemical properties to enhance its performance as electrode material [70].

2.2. Pyrolysis

Pyrolysis usually produces activated carbon (AC) at temperatures below 1000 °C [71]. Pyrolysis conditions (mainly temperature) play a significant part in creating the AC's surface and textural features. Increasing the temperature resulted in increasing the graphitization and thus decreasing the surface's electrical resistance. Studies have also shown that higher pyrolysis temperature contributes to the pore's growth by eliminating part of the volatile matter, thereby increasing the micropore-associated surface area. A flexible carbon sponge derived from cotton was synthesized via pyrolysis and NH_3 treatment at high temperatures (750–1100 °C). The resulting electrode displayed a high SSA up to 2680 m^2/g, a specific capacitance of 110 F/g, and an excellent desalination performance (16.1 mg/g). Fly ash of sugarcane bagasse was used to prepare AC by a thermal treatment between 200 and 800 °C, which was used to fabricate a CDI electrode. High temperature, 800 °C, immensely increased the SSA from 226 to 463 m^2/g while low temperature, 200 °C, exceeded the surface oxygen groups; thus, the electrode wettability. The improved wettability at low temperature resulted in increasing the salt adsorption capacity (6.2 mg/g).

2.3. Activation

The activation process plays an essential role in increasing porosity and enhancing the SSA of carbon materials [72]. The activation can be done by chemical means in an inert environment at a specific ratio of the activating agent to the carbon, by physical means (CO_2 or steam), or both [63]. Physical activation is more straightforward and environmentally driven than chemical activation; however, it requires a higher temperature (800–1000 °C) and longer activation time. Physical activation using carbon dioxide increases the average pore volume. While chemical activation creates activated carbon with a high SSA, good porous structure, a wide distribution of pores, and high carbon content. However, chemical activation had many significant drawbacks, including a post-activation water washing process required to eliminate impurities and additional treatment necessary to handle polluted water byproduct [73]. Potassium hydroxide (KOH) is the frequent chemical medium used for biochar activation. Zinc chloride ($ZnCl_2$) is also used as a chemical agent for activation [74]. Compared with KOH activation, CO_2 exhibits a high level of graphitization for capacitive deionization and energy storage applications [75]. The activation temperature is a crucial factor in the resulting physicochemical characteristics of the carbon material. A porous carbon with high SSA was prepared from chicken feathers [76] and activated chemically using different KOH:C ratios at different temperatures. The SSA of the untreated carbon was 642 m^2/g which significantly increased to 1642 m^2/g after activation with KOH at 800 °C.

2.4. Salt templating

Salt templating is an efficient and straightforward route to produce porous carbon materials doped with heteroatoms. A heteroatoms' precursor is applied to the activated carbon/biobased materials and mixed with a low melting point salt to enable heteroatom doping into the produced carbon. Low melting point salts like LiCl, NaCl, KCl, or $ZnCl_2$ that behave as both solvent and template are used [77]. This technique is employed to fabricate carbons doped with a heteroatom, adjustable pore volume and structure, and a high surface area. Such properties cannot be realized through conventional activation methods. The salt template's addition stabilizes the pore structure, prevents the formation of carbon bumps and clusters, and creates an ordered structure during hydrothermal [78]. The heteroatoms such as boron, phosphorus, nitrogen, and sulfur enhance the electrical conductivity and wettability, leading to improved electrochemical performance. Nitrogen is the most used doping agent due to its similar atomic size and valence bonds to carbon. Nitrogen-doped carbon has a higher content of defects, higher accessible area, and higher sites for charge adsorption, thereby improving the capacitance. A biomass-based carbon precursor was fabricated from glucose, glucosamine, and 2-thiophene carboxylic acid "as a sulfur source". Zinc chloride and cesium acetate were used as a salt template and an activating agent. The obtained carbon demonstrated a high SSA of 2830 m^2/g (1.0 mass% N) with a high sorption capacity of 15.0 mg/g. Fig. 2 shows a comparison of the different preparation methods in terms of advantages and disadvantages.

3. Bio-based electrodes in CDI for water desalination

The most crucial application of CDI systems is water desalination, where the CDI cell is used to adsorb sodium and chlorine ions from the water, thus reducing the water salinity. In this section, implementing bio-based materials for preparing CDI electrodes for water desalination is summarized and discussed.

3.1. Agriculture-based electrode materials

This section summarizes the progress done in preparing activated carbon using different agricultural residues for CDI.

Cotton: Cotton-derived carbon sponge obtained by the pyrolysis of raw cotton was prepared at different heat temperatures (750, 850, 950, 1100 °C) under ammonia and applied as an electrode of the CDI cell. The highest performance was obtained at 1000 °C, with an electrode's specific capacitance of 109.9 F/g with a high charge efficiency of 77 %, and an electrosorption capacity of 16.1 mg/g using an initial NaCl solution of 500 mg/L [79]. Moreover, the electrode showed good cyclic stability and high reversibility adsorption/desorption. The excellent performance of the cotton-derived carbon sponge electrode was related to its high SSA of 2680 m^2/g, excellent electrical conductivity, suitable pore size distribution (0.8–4 nm), and high hydrophilicity (due to the plenty of oxygen surface groups).

Sugarcane bagasse: Sugar cane bagasse is commonly used as boiler fuel, underestimating its value compared with its chemical-driven materials. Using microwave-assisted carbonization, bagasse was used to prepare hierarchically porous biochars followed by activation (using potassium hydroxide in CO_2 and N_2). The produced biochars are tested in CDI cells under different flow rates ranging from 100 to 600 cm^3/min. The total pore volume ratio of the bagasse-based biochar activated under a CO_2 flow of 300 cm^3/min (CO_2-300) was 56.7 % compared with 45.4 % in the N_2-600 electrode. Moreover, the CO_2-300 showed higher mesopore volume, higher SSA (1019 m^2/g), and thus a higher specific capacitance of 208 F/g at 5 mV/s, compared with 96 F/g for the N_2-300 biochar. The desalination tests at 1.2 V in a batch mode using a 5 mM NaCl confirmed that the CO_2-300 had an excellent electrosorption capacity of 28.9 mg/g and a faster salt rate adsorption than N_2 activated samples. The salt absorption capacity (SAC)

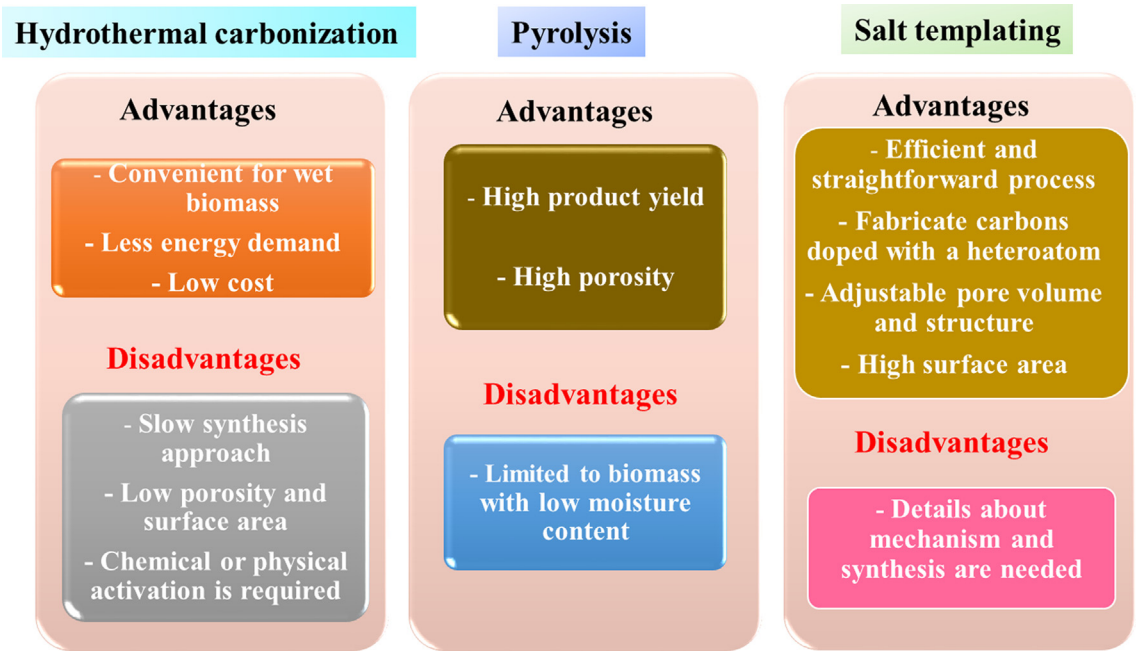

Fig. 2. Advantages and disadvantages of the different biochar preparation methods.

observed for all CO_2-x samples was significantly higher than those of N_2-x samples [80]. A sugarcane bagasse fly ash (SCBFA) was used to synthesise AC via the pyrolysis process. Increasing the pyrolysis temperature increased the surface area by removing part of the fly ash, while pyrolysis at a low temperature,200 °C, prevented the decomposition of surface oxygen groups (SOG) that are responsible for the electrodes' wettability. The SCBFA-based ACs were investigated as CDI's electrodes, higher specific capacitance values at 1 mV/s were obtained at 200 °C (55 F/g) and 400 °C (39 F/g) compared to the lower values at higher temperatures at 600 °C "34 F/g" and 800 °C "20 F/g" and the maximum salt adsorption capacity was 5.3 mg/g at 200 °C. SCBFA-based AC was synthesized by chemical activation of SCBFA using $ZnCl_2$ or KOH as activation agents. Using a high mass ratio of $ZnCl_2$ (>1:2) decreased the SAC regardless of activation temperature due to residual Zn's existence and thus reduced the electrosorption. Although more profound cleaning decreased the amount of residual Zn, it was not adequate to remove all Zn from the AC [81]. Thereby, SCBFA chemically activated with $ZnCl_2$ is not proper for CDI's electrode. On the other hand, using KOH as activating agent drastically decreased the carbon hydrophobicity, which in terms enhanced the polar surface oxygen group (SOG), increasing the SSA, thus improving the specific capacitance of AC and increasing the SAC values. SCBFA was physiochemically activated using KOH and CO_2 to acquire AC with more mesopores, more SOG, and higher surface area [82]. The combination of physical and chemical activation significantly improved the properties of the synthesized AC. The physiochemically activated AC was used as CDI electrode showing a higher electrochemical performance than AC produced chemically or physically. This was related to the higher SSA (18.5–20.5 mg/g) and more mesopores of AC that resulted in hastier salt adsorption kinetics and long term stability as 87 % of SAC remain after 70 cycles.

3.2. Rice husk:

Rice husk (RH) is common agricultural biomass, with a global 148.2 million tons in 2014 [83,84]. A HPC "hierarchical porous carbon" electrode from rice husk biochar was prepared and compared with commercial activated carbon powder (F400) [85]. The HPC showed a SSA of 1839 m^2/g with a higher mesopore volume to a total pore volume ratio of 0.58 compared to 0.48 of the commercial activated carbon. The HPC electrode's specific capacitance was 120.5 F/g at 5 mV/s, indicating a high ability to store capacitive ions. The HPC's electrosorption capacity was 8.11 mg/g, and a 0.92 mg/g/min deionisation rate was achieved. The energy consumption in the case of the HPC was found to be 0.064 kWh/mol, which is lower than that consumed in the case of F400 (0.082 kWh/mol). Furthermore, the HPC showed an excellent regeneration capacity, indicating its suitability for water desalination and other water softening applications and treating ammonium and heavy metal contaminated water. Activated carbon (AC) derived RH was also prepared through carbonization under different temperatures (350, 450, 600, and 750 °C) [86]. The synthesized RHAC was examined in CDI. The RHAC prepared at 450 or 600 °C showed higher salt removal efficiency due to their high SSA and mesopore volume. The RHAC synthesized at 600 °C achieved the highest desalination performance as 5.2 g of salt per g of electrode per day.

Moreover, the electrode almost maintained its electrosorption capacity and kinetics after 80 electrosorption/desorption cycles. RH-AC was also prepared by carbonization under a nitrogen atmosphere at 500 °C followed by chemical activation using KOH under a nitrogen atmosphere at 800 °C using the mass ratio of KOH to the precursor of 4:1 [87]. The prepared RH-AC exhibited an SSA of 2290 m^2/g and showed a superior electrosorption capacity of 20.02 mg/g. HPC-derived RH was synthesized by the carbonization process followed by steam activation in the existence of silicon components working as a natural template to control the hierarchical porous structure (RHC-A). Finally, the RHC-A was treated with hydrofluoric acid to remove the silicon component, obtaining mesopore-dominant porous carbons (RHC-H) [88]. RHC-A and RHC-H were investigated in CDI under batch and continuous modes to recognize the pore structure's influence on CDI performance. RHC-A and RHC-H showed lower maximum electrosorption than commercial AC under batch mode. While under the continuous mode, RHC-A attained the highest salt removal capacity (8.09 mg/g) compared to RHC-H (1.63 mg/g) and commercial AC (5.4 mg/g). The RHC-A promoted the ions adsorption and trans-

portation due to the interconnection between mesopores and micropores structure.

Shiitake *(Lentinus edodes)* mushroom: *Lentinus edodes* is an edible mushroom that is cultivated and consumed in many Asian countries.

The performance of the CDI unit using untreated carbon (UC) and $ZnCl_2$ treated carbon (TC) derived from hydrothermal treated *Lentinus edodes* was compared to that using activated carbon (AC) using 500 ppm NaCl, a constant flow rate of 10 mL/min, and 1.2 V [89]. The specific capacitance and salt absorption capacity (SACs) for UC, TC, and AC electrodes were 232 F/g, 247.6 F/g; 198 F/g, 9.24 mg/g; 12.9 mg/g, and 6.6 mg/g, respectively. These results showed the positive effect of $ZnCl_2$ activation on the biomass electrode, reaching a maximum efficiency of 65.7 %.

Soybean: NPC "Nitrogen-doped porous carbon" and its sulfonated one (S-NPC) were produced from soybean shells using pyrolysis followed by $KHCO_3$ treatment in N_2 atmosphere and aryl diazonium salt mixture with sulfonic groups. The SSA and total pore volume of NPC and S-NPC were 1036.2 and 844.0 m^2/g; and 0.43 and 0.37 cm^3/g, respectively. The sulfonic groups effectively reduced the expulsion impact of the co-ions. They improved the charge efficiency, the specific capacitance (215.3 F/g for S-NPC and 165.2 F/g for NPC), and the SAC (16.0 mg/g for S-NPC and 15.5 mg/g for NPC). The adsorption and desorption rates for S-NPC electrodes were also higher than those of NPC [46]. Soya bean was also used to synthesise NAPC/G "*N*-doped activated porous carbon decorated by graphene" [90]. The soya beans were crushed with a ball mill, stemmed for 30 min at 90 °C; then, the mixture was sieved to attain soy milk [90]. The NAPC/G was obtained through pre-carbonization and chemical activation using KOH. The NAPC/G electrode realized a high specific capacitance of 370 F/g and high stability as the electrode maintained 97 % of its capacitance after 3000 cycles. Moreover, NAPC/G attained a promising SAC of 38.5 mg/g, a desalination rate of 6.6 mg/g min and high stability as the desalination performance maintained 93.5 % after 50 cycles. The superior performance of NAPC/G-based CDI was related to the ultra-high SSA (2993.5 m^2/g), high hydrophilicity, and prolific micro-mesoporous structure of NAPC, in addition to the high conductivity of graphene.

Bamboo: A composite synthesis of bamboo-based activated carbon (BAC)/manganese dioxide (MnO_2) was tested in a CDI system. The results showed BAC has an outstanding electrical conductivity, a large surface area of 1747 m^2/g, a hierarchical pores structure, and a capacitance of 158 F/g at 10 mV/s. Furthermore, the specific capacitance does not decrease even after 500 cycles, and all charge–discharge graphs displayed well triangular and symmetrical shapes indicating good cycling stability and reversibility. Large quantities of surface oxygen groups increased the whole composite's hydrophilicity, whereas the MnO_2 nanoparticles offered a high adsorption capability and rapid reaction kinetics. CDI tests carried out in 150 mL NaCl solution at 1.2 V showed a SAC of 10.3 mg/g [91].

Palm tree: *Phoenix dactylifera*, or a date palm tree, is an abundant supply of solid agricultural waste, mainly seen in the world's arid and semiarid areas. A study by Govindan et al. [92] proved the effectiveness of activated carbon electrodes derived from the leaf of palm tree waste. The electrodes' modification allowed a reversible intercalation/transition of Na ions by the involvement of nanoscale α-MnO_2 particles appearing as redox mediators. For the functional composite substance (α-MnO_2/f-AC), the α-MnO_2 nanoparticles (NPs) are produced hydrothermally on the activated carbon powder (Fig. 3 (a)). The pristine α-MnO_2/f-AC has a specific area of 1224 m^2/g and electrical capacitance of 259 F/g at 10 mV/s. The CDI electrodes' desalination performance was evaluated using α-MnO_2/f-AC, and f-AC derived electrodes as anode and cathode, Fig. 3 (b). Results demonstrated electrosorption capacity of 17.8 mg/g using 600 mg/L NaCl batch-mode CDI; an electrochemical adsorption rate of 1.7 mg/g/s, and SAC retention higher than 99.7 %. These results suggest that the electrodes centred on α-MnO2/f-AC // f-AC can be reliable and stable for CDI applications (Fig. 3 (c)). The CDI cell's improved electrical efficiency and pseudocapacitive activity can be described by the α-MnO_2 nanoparticles playing a significant role in promoting synergistic redox-based charge–discharge direction conditions that are consistent with the CDI process's voltage operating requirements.

Date palm leaflets were chemically activated using NaOH to synthesise AC and investigated as an electrode in CDI under different applied voltage (1, 1.2, 1.4, 1.6 and 1.8 V) and salt concentrations (50, 100, 200 and 300 mg/L) [93]. It revealed that the SAC was influenced by the amount of mesopores found in the AC, and the highest SAC of 5.38 mg/g was achieved using 100 ppm NaCl solution at 1.8 V. A natural palm tree was chemically activated to fabricate a 3D microporous graphene-like carbon (CNPT) [94]. Then CNPT was mechanically mixed with multi-walled vanadium oxide nanotubes (*VO_x NTs*), 5 wt%, to form a *VO_x NTs /CNPT* composite and investigated as cathode for hybrid CDI. A *VO_x NTs /CNPT* cathode exhibited an ascendant salt adsorption retention of 94.7 % after 50 charge/discharge cycles. Shell wastes discarded from the processes of extraction of palm and bitter tea oil yield small amounts of sulfur, nitrogen, and toxic compounds. At the same time, carbon can be used to manufacture low-cost ACs. Bitter-tea and palm shell waste products were used as base materials to form activated carbons, then applied in the CDI. The palm-derived activated carbon (PAC) was also doped with Ag^+-cyclodextrin complexes (Ag@C/PAC) at 673 K. At 1.2 V, an electrosorption efficiency of 25 % was obtained in the case of the bitter tea-derived activated carbon (BAC) compared to 28 % in the case of the PAC electrodes. Reversing the polarity of PAC and Ag@C/PAC from 1.6 V to −1.6 V improved the electrosorption efficiency by 40 %. After 20 cycles, both doped and undoped electrode materials are stable in CDI operation. The Ag@C/PACs demonstrated a high disinfection ability (95–98 %) for two hours [95].

Dates: Dates are among the most abundant biomass resources in regions with large deserts, such as the Middle East and North African countries. Biochar produced from date seeds was used for porous activated carbon synthesis using KOH, Fig. 4a. Date seed-derived-derived activated carbon (DSAC) porosity increased with increasing biochar/KOH ratios. The maximum specific surface area was obtained at a ratio of 1:1.5 (1020.85 m^2/g) compared to values of 579.35, 803.65, and 980.55 m^2/g for ratios 1:0.5, 1:1, and 1:2, respectively. The specific capacitance values at a 10 mV/s were 180 F/g for ratio 1:0.5, 275 F/g for ratio 1:1, 100 F/g for ratio 1:1.5, and 340 F/g for the highest ratio of 1:2. The maximum charge efficiency was obtained at the 1:1.5 ratio (86.4 %) in comparison to 1:0.5, 1:1, and 1:2, where the respective charge efficiencies were 61.6 %, 70.1 %, and 74.2 %, respectively. Furthermore, the biochar/KOH ratio of 1:1.5 demonstrated the maximum deionizing capacity, the fastest electrosorption rate (Fig. 4 b & 4c), and an electrosorption capacity of 22.2 mg/g, which is better than many reported commercial electrodes. It was also found that the electrode with a ratio of 1:1.5 had an excellent regeneration performance with up to 6 batch cycles with negligible electrosorption capacity loss (<5%) [96]. A binderless AC monolith was fabricated from date stone by pyrolysis process under nitrogen atmosphere at 1000 °C (CP1000) followed by physical activation under CO_2 at 900 °C (ACP900) [55]. The physical activation significantly increased the SSA from 248 to 877 m^2/g, and the microporosity structure was well developed. The ACP900 was investigated as a CDI electrode exhibiting high specific capacitance of 270.9 F/g at 10 mV/s.

Lotus leaf: An abundant yet discarded carbon source, just 1 % of the 70–100 M tons of lotus leaf (LL) available in China is currently

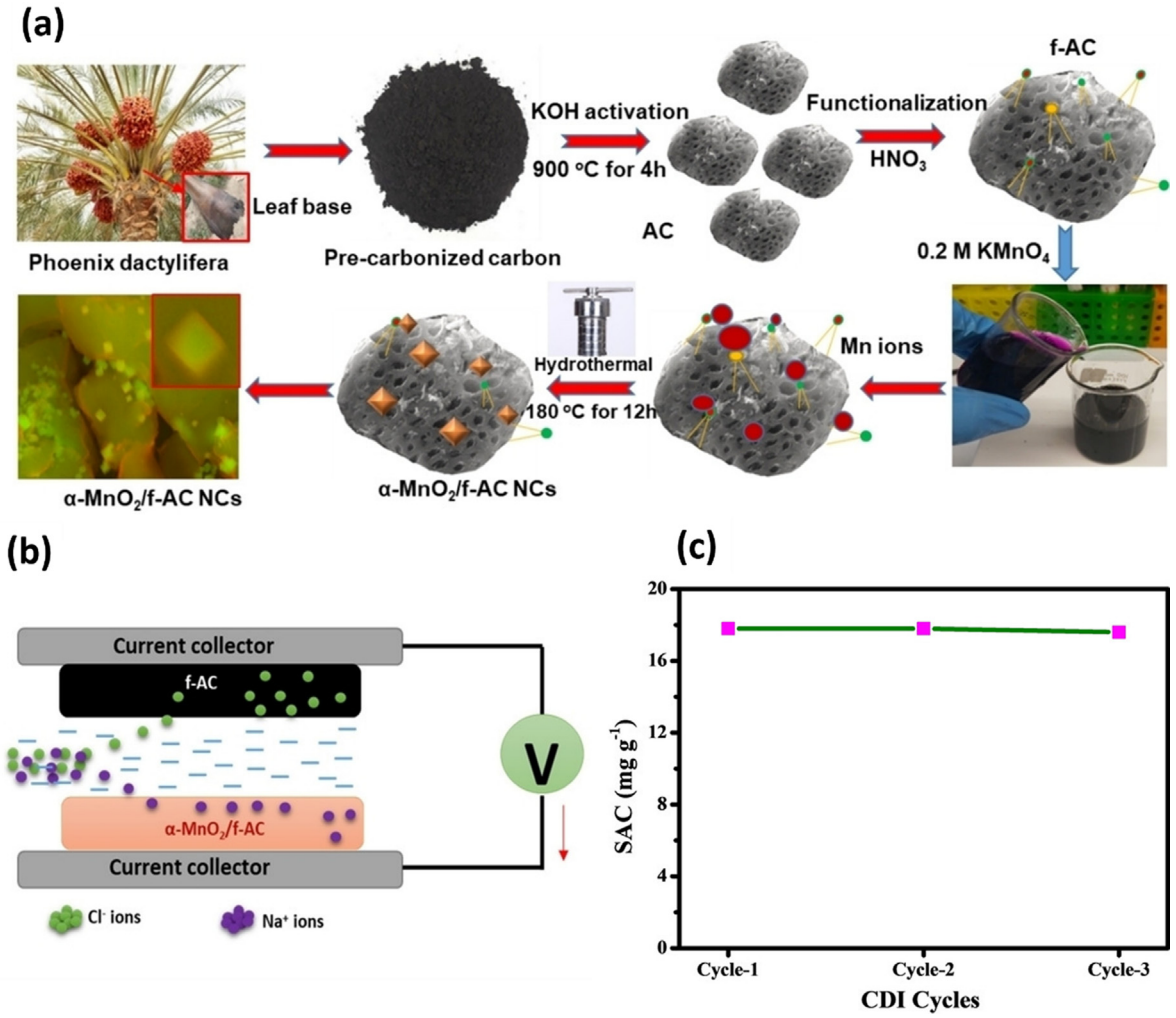

Fig. 3. (a)The fabrication procedure of α -MnO_2/f-AC electrode material, (b) The asymmetric CDI cell structure used, (c) The salt adsorption capacity for first three cycles in a 600 mg/L NaCl sol. and 1.2 V, adapted from [92], open access.

being used, mostly in the catering industry [97]. Hydrophilic porous carbon nanosheets with SSA of 4482 m^2/g were developed using lotus leaf. The nanosheet-specific capacitances were 225 F/g and 289 F/g at 0.5 A/g in 1 M NaCl and 6 M KOH solutions. The electrosorption capacities were 13.5 mg/g and 65.0 mg/g towards NaCl at 1.2 V and 1.6 V. The conductivity recovers to the initial amount even after 10 cycles, indicating the activated LL electrode has good reversibility [98]. Lotus stems were used to fabricate a 3D tertiary porous electrode via a carbonization process at 500 °C pursued by activation at 800 °C, LS500/A800 [99]. The LS500/A800 had a hierarchical macro-, *meso*-, and micro-porosity, "a tertiary pore structure". The synthesized electrode was examined in MCDI cell and achieved a SAC of 31.7 mg/g at 1.4 V and high stability (97 % SAC remained after 100 cycles). The high desalination performance and stability of LS500/A800 electrodes based MCDI related to the high surface area (2500 m^2/g), high porosity and robust framework of the tertiary pore structure electrode that enhanced the ion adsorption and introduced more adsorption sites.

Pine: Phosphorus-doped porous carbon was manufactured by activation of pinecones (PPCP), an abundant agricultural waste, using H_3PO_4 as the activation agent at different activation temperatures (700, 800, and 900 °C) [100]. The PPCP electrodes increased the pore's SSA and volume while increasing the activation temperature. PPCP treated at 800 °C (PPCP800) and 900 °C (PPCP900) have specific areas of 1176 m^2/g and 2034 m^2/g, and pore volumes of 0.45 cm^3/g and 0.81 cm^3/g, respectively. While the PPCP800 electrode does not have the largest SSA, its specific capacitance ranks the best of all the electrodes due to the high degree of graphitization, superior porous nature, the highest phosphorus content, and the smallest charge transfer resistance. The PPCP800 electrode showed the highest salt removal capacity of 14.62 mg/g at 1.2 V using 1000 mg/L NaCl sol. with the highest salt removal rate. PPCP800 electrodes also showed no degradation in desalination performance during the first 100 cycles, suggesting good repeatability [100].

Pine pollen, a natural and abundant material rich in cellulose, was utilized to produce porous carbon materials [101]. The porous material formed by calcination at 900 °C resulted in salt removal capacities of 7.25 mg/g and 19.43 mg/g at NaCl solution of 50.5 mS/cm and 500 mS/cm, respectively. The electrode also offered good process stability due to its large SSA and pore volume. The low surface oxygen concentration decreased the material's ohmic resistance and increased the charge efficiency [102]. This result contradicts the improvement of the CDI performance by the oxygen surface groups due to their role in enhancing wettability.

Peanut: Peanut crops are widely distributed around the world. Activated carbon with low ash content and high porosity could be obtained through carbonization of peanut shells followed by alkali activation at 750 °C. A CDI desalination system using Peanut derived activated carbon (PS-AC) demonstrated a better perfor-

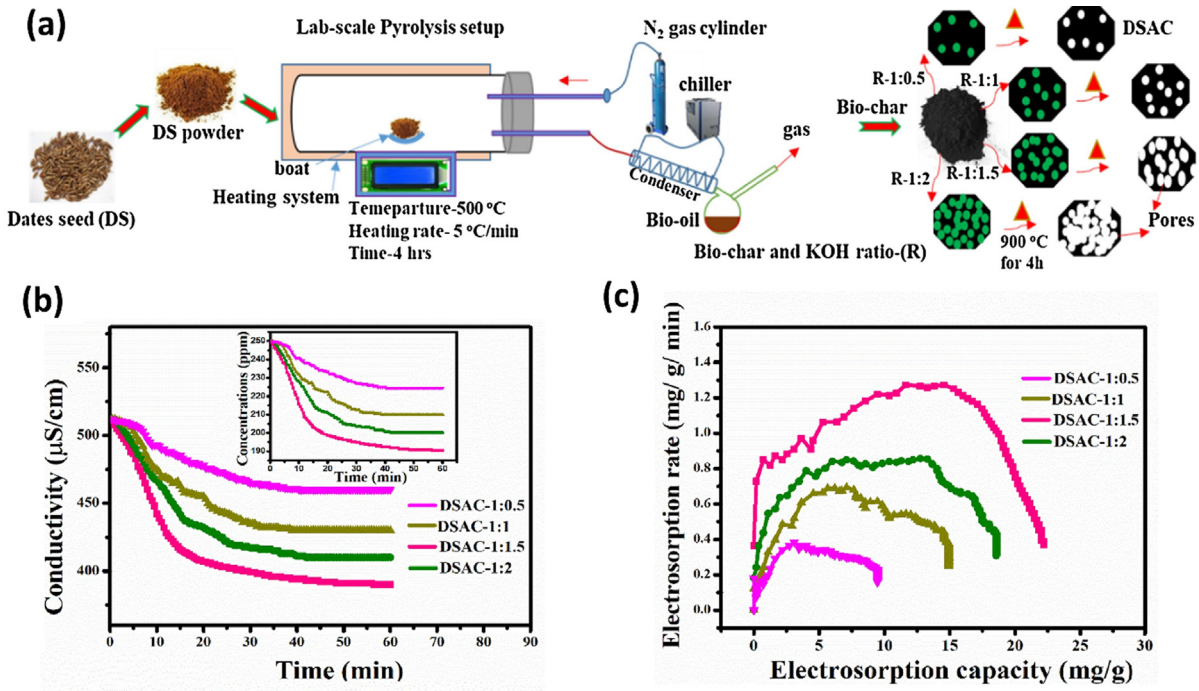

Fig. 4. (a) Schematic of date seed activated carbon using pyrolysis, (b) Desalination experiment results at 250 mg/L and 1.2 V, and (c) CDI Ragone plots for the synthesized activated carbon electrodes, adapted from [96], with permission No. 5414201279912.

mance than commercial activated carbon used in supercapacitors (SC-AC) due to the defects and the larger pore size of the PS-AC. The introduction of thermally treated MoS_2 (D-MoS_2) into the PS-AC improved the performance. The maximum specific salt-adsorption capacity of the D-MoS_2/PS-AC system was 8.98 mg/g for CDI experiments at 1000 mg/L of initial NaCl at 1.2 V, compared to 7.92 mg/g for PS-AC/PS-AC. The PS-AC/SC-AC electrodes showed a salt removal percentage of 28.7 %, and the D-MoS_2/PS-AC showed a salt removal percentage of 35 %. The improved performance using D-MoS_2 was related to the shorter deionizing cycle time and a greater electrosorption capacity of MoS_2 due to its negatively charged surface that attracts more ions [103].

Almond: Three different activated biochar carbons under three pyrolysis temperatures from raw almond shells were investigated as electrodes for a CDI system with a 500 mg/L NaCl sol. at 1.2 V. The specific surface area at 900 °C (452.2 m^2/g) is almost double that at 800 °C (226.3 m^2/g); however, increasing the temperature to 1000 °C resulted in a decrease of approximately 30 % to 317.4 m^2/g. 900 °C showed the best performance with 19.2 mg/g SAC ion adsorption. The energy consumption reported was 0.26 kWh/m^3, making it competitive with conventional brackish water desalination systems [49].

Loofa sponge: Loofa sponge (*Luffa cylindrica*) composed of approximately 60 %, 30 %, and 10 % of cellulose, hemicellulose, and lignin, respectively, was used as a base material for the fabrication of activated carbon by pyrolytic carbonization. A hierarchically porous structure was obtained after activation with KOH, where the total SSA, specific capacitance, and the total pore volume increased with increasing alkali/char ratio. The Loofa sponge (LS) derived carbon prepared using 4:1 of KOH/char demonstrated the highest adsorption capacity of N_2 with a SSA of 1819 m^2/g. A specific capacitance of 93.0 F/g at 5 mV/s in an aqueous solution of 1 M NaCl. Furthermore, the electrosorption capacity was 22.5 mg/g in batch CDI at 1.0 V when using 10 mM NaCl. The corresponding ion removal efficiency was 40.1 %, and the recovery rate was 97 % [104]. Luffa sponge was carbonized at 800 °C under Ar atmosphere to obtain Luffa-derived carbon (SDL-C), then chemically activated using KOH at 800 °C (SDL-A) [105]. Luffa-derived carbon before and after activation was investigated as electrodes in a batch mode MCDI under different salt concentrations (500 to 2500 mg/L) and applied potential (0.8–1.2 V). SDL-A exhibited a higher SAC of 38 mg/g using 2500 mg/L NaCl and 1.2 V compared to SDL-C (22 mg/g). Moreover, SDL-A showed lower energy consumption of 132 kJ mol^{-1} salt in comparison of SDL-C (143 kJ mol^{-1}). Outstanding SAC of SDL-A related to the existence of micro/mesoporous structure formed during the activation process.

Coconut: Huynh et al. [106] studied the performance of an innovative composite of CNTs and activated carbon derived from coconut shells as CDI electrodes. The surface area of the electrode with a mass ratio AC/CNT of 9:1 was recorded at 630 m^2/g, with a specific capacity of 90.2 F/g at 20 mV/s, a SAC of 14.1 mg/g at 1.0 V, and energy consumption of 0.312 kWh/m^3. The addition of CNTs to the AC enhanced the overall electrode's electrical and electrochemical performance while maintaining good mechanical properties and stability, with 100 % capacitance reserved after 10 cycles. Another study activated biochar (AB) extracted from coconut shells combined with manganese dioxide for CDI applications. The AB-MnO_2 nanocomposites, developed by indirect co-precipitation, exhibited a specific surface area of 304 m^2/g with specific capacitance in the range of 410–523 F/g at 5 to 200 mV/s. The specific electrosorption capacity was 33.9–68.4 mg/g at solution concentrations ranging 100–1000 mg/L. Ultimately, the nanocomposite displayed good electrochemical reversibility, excellent regeneration performance, and electrochemical stability [107]. Coconut shell-derived activated carbon (CS-AC) was synthesized hydrothermally at 850–950 °C. Graphene, carbon nanotube or both (1 wt) was incorporated in CS-AC, constituting three different electrodes named AC/Gr, AC/CNT, or AC/Gr/CNT, respectively [108]. The synthesized electrodes were investigated for CDI desalination of brackish water. Among different electrodes, AC/Gr/CNT realized the highest desalination performance due to the synergistic effect

of the graphene and CNT, achieving salt adsorption rate of 1.51 mg/g min (at 1.0 V), SAC of 9.58 mg/g and capacitance of 60 F/g (at 5 mV/s) in 200 ppm NaCl, Fig. 5.

Tamarind: Tamarind shell was used to fabricate two-dimensional *N*-doped porous carbon nanosheets activated with KOH. The *N*-doped nanosheet surface area was 410 m^2/g, and its specific capacitance was 174.5 F/g at 10 mV/s compared with 70.6 F/g for the undoped carbon. The salt adsorption capacity tested in a 600 mg/l NaCl medium at 1.2 V was 18.8 mg/g in the *N*-doped nanosheets, which is significantly larger than undoped carbon (11.1 mg/g). The charge efficiency (CE) at 1.2 V was 83 % for the doped material than the undoped carbon's CE value of 71 %. The *N*-doped carbon greatly enhanced the electrode's wettability and improved the electrosorption performance due to smaller ion transfer and high active sites, making it an excellent electrode material for the effective CDI process [109].

Jackfruit: A high surface area porous carbon was synthesized by carbonizing agricultural waste jackfruit's peels, followed by KOH activation [110]. The activation process significantly increased the synthesised carbon's SSA from 607 m^2/g to 1955 m^2/g. The activated electrode had the highest specific capacity of 307 F/g, the highest salt removal efficiency of 95 %, and the highest electrosorption capacity of 1.18 mg/g on batch desalination tests with 30–500 mg/L NaCl using 2.5 mL/min at different voltages of 1.2, 1.4 and 2.0 V.

Citrus: Citrus peels are rich sources of polysaccharides, making them a suitable-based material for carbon electrodes. A hydrothermal synthesis process was used to prepare carbon material for electrodes from the citrus peel, and the effect of $ZnCl_2$, KOH, and H_3PO_4 additives was studied. The $ZnCl_2$ addition enriches the functional groups containing O and N and provides a higher SSA of 323 m^2/g than 265 m^2/g and 25 m^2/g for KOH and H_3PO_4 addition, respectively. $ZnCl_2$ activated carbon also displayed the highest specific capacity of 120 F/g. When used as an anode in the CDI cell, a desalination removal of 16 mg/g and a salt adsorption rate of 0.67 mg/g/min was obtained, higher than values corresponding to KOH and H_3PO_4 activated electrodes. $ZnCl_2$ electrode has the highest charge efficiency of 61.4 % and an 80 % desalination retention after 35 cycles [111].

Watermelon: The behavior of activated carbon derived from watermelon (WMAC) was investigated as an anode and its composite (WMAC/$MnFe_2O_4$) as a cathode in a CDI system for desalination [112]. WMAC was developed by H_3PO_4 activation via single-step low-temperature pyrolysis. The SSA and the total pore volumes for WMAC and WMAC/$MnFe_2O_4$ were 618 m^2/g and 483 m^2/g, and 0.902 and 0.736 cm^3/g, respectively. The composite high specific capacitance of 425 F/g was linked to the pseudo-capacitance synergistic effect and the influence of MnFe2O4 and the electric double layer. Desalination experiments conducted using 50 mL of NaCl, 10 mL/min, and 1.2 V, revealed a high nanocomposite's electrosorption capacity of 29 mg/g, good recyclability, and fast desalination. A 93 % retention of ion uptake with a 5.5 % decrease in charge efficiency was observed after 4 cycles.

3.3. Animal-based electrode materials

In this section, progress was made in using animal-based material to prepare activated carbon.

Eggs: *N*-doped porous carbon obtained from egg whipped foam, i.e., activated egg whipped carbon (AEWC) by freeze-drying and secondary carbonization (Fig. 6 (a)) demonstrated a specific capacitance of 136.61 F/g compared to 92.49 F/g in the case of commercial supercapacitor activated carbon (SCAC) (Fig. 6 (b)). AEWC also had a unique micro-mesoporous structure with an outstanding SSA of 3277.96 m^2/g and a total pore volume of 1.41 cm^3/g compared to 2032.27 m^2/g and 0.88 cm^3/g for commercial SCAC. The AEWC electrode achieved a high salt adsorption capacity of 26.67 mg/g compared to 16.01 mg/g for SCAC and a rapid salt adsorption rate at 1.2 V batch mode in 500 mg/L NaCl solution (Fig. 6 (c)). Furthermore, the specific capacitance and shapes of CV curves using the AEWC barely altered after 2000 cycles, demonstrating strong cycling stability. Moreover, after five regeneration cycles had been completed, the AEWC electrode's salt adsorption capacity is still

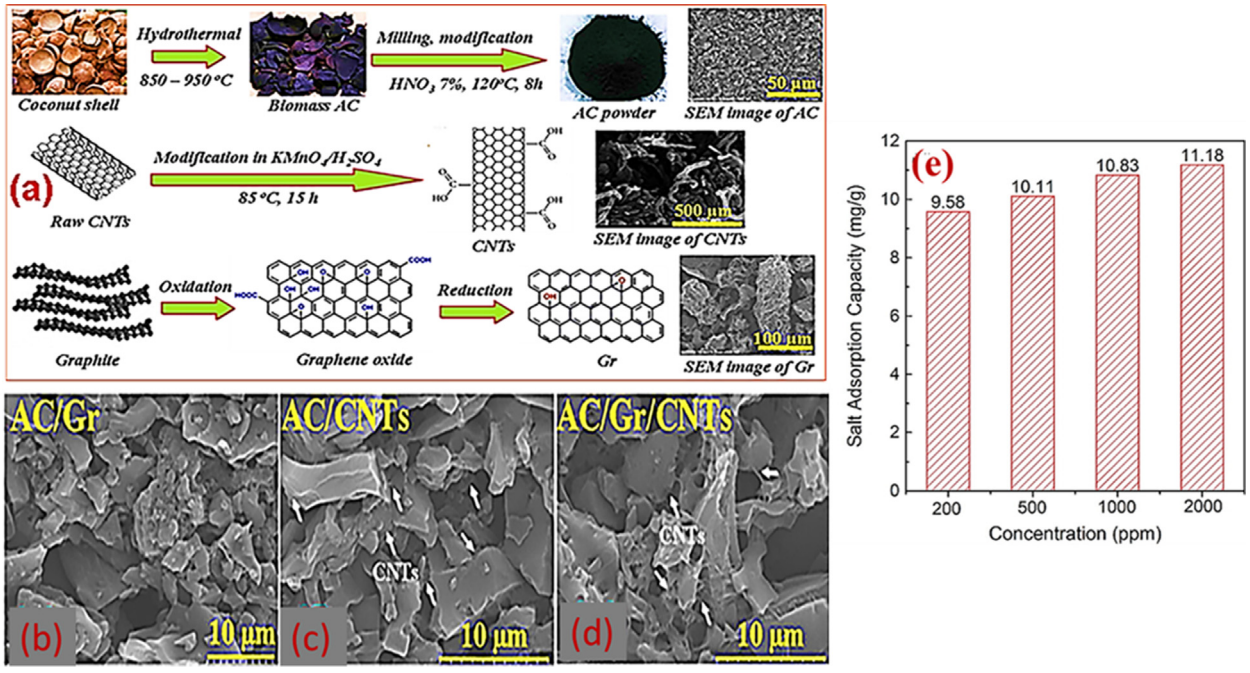

Fig. 5. (a) Preparation of AC, CNTs, Gr; (b) FE-SEM image of AC/Gr (c) FE-SEM image of AC/CNTs; (d) FE-SEM image of AC/Gr/CNTs, (e) the influence of NaCl concentration on SAC of different electrodes [108] with permission No. 5414201510093.

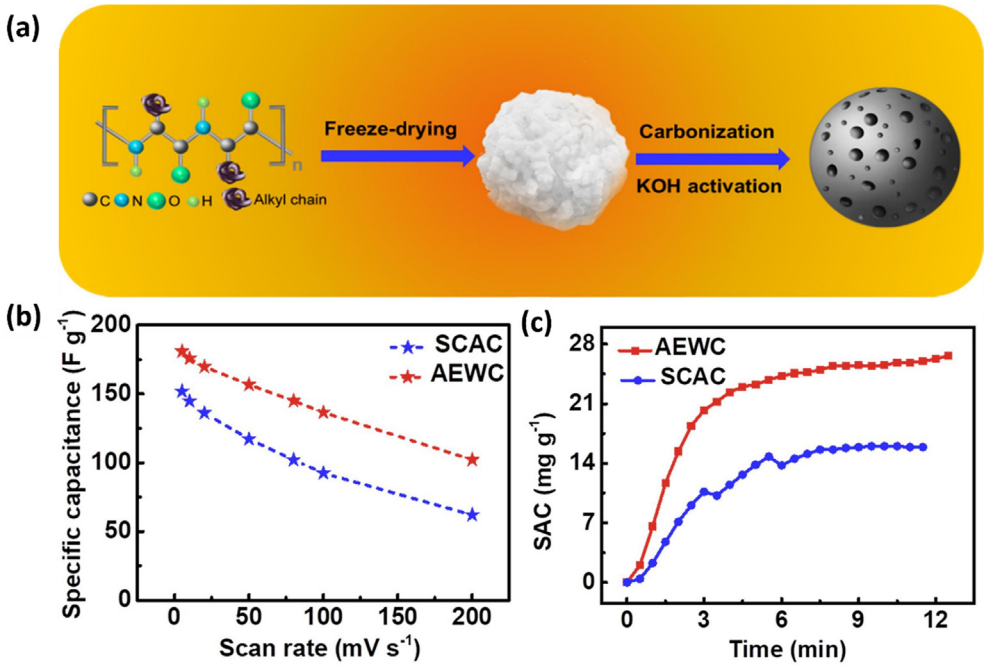

Fig. 6. (a) Fabrication process of the *N*-doped porous activated egg whipped carbon (AEWC) foam, (b) specific capacitance of the doped egg white carbon compared to commercial supercapacitor carbon (SCAC), (c) salt adsorption performance of both materials, adapted from [113], reproduced with Permission No. 5414291168437.

well-preserved, suggesting strong desalination process reversibility [113].

Leather: Leather consists more than 80 % of collagen which has a high proportion of heteroatoms and a low ash concentration. A carbon aerogel was prepared through a one-step pyrolysis-activation by KOH treatment of leather waste. The leather waste-activated carbon (LWAC) has a SSA of 2523 m^2/g and a specific capacitance of 97.57 F/g at 10 mV/s; these values are significantly higher than commercialised ACs (1425 m^2/g and 5.62 F/g, respectively). For a solvent volume fixed at 80 mL, 10 mL/min, and 1.2 V, the adsorption capacity of LWACs at a concentration of 500 mg/L was 20.92 mg/g which is 7.4 times greater than that of commercial ACs (2.82 mg/g). Furthermore, the specific capacitance of the LWACs remained mostly unaltered after 1000 cycles, demonstrating excellent cycling stability. The one-step pyrolysis-activation method for electrode synthesis from LW would significantly contribute to the CDI system's economic efficiency [114].

Chitosan: Chitosan, an abundantly available polysaccharide derived from shellfish [115], was used for the production of chitosan-based activated carbon (CTSAC) for use as CDI electrodes [116]. The electrode was produced by pyrolysis, followed by KOH activation. The CTSAC retained 10–30 % of the heteroatom material, mostly from the chitosan amino and hydroxyl groups. The resulting SSA was 2727 m^2/g, and the electrical conductivity was 2.09 S/cm. The results of the CDI indicated a salt absorption capacity of 14.12 mg/g in a 500 mg/L NaCl aqueous solution and a 95 % capacity retention after 150 cycles of adsorption–desorption. At 1 A/g, the CTSAC's specific capacitance was 185 F/g; however, at 100 A/g, the capacity retention rates dropped 54 %. A 3D cross-linked chitosan (CS) was fabricated with different glutaraldehyde content (GA) of 0, 1, 3, 5, and 10 wt%) named CS + xGA [117]. The AC was coated with CS + xGA and tested as anodes of asymmetric CDI cells, while CS + PVDF (Polyvinylidene Fluoride) was used as a cathode. Among the different anodes, CS + 3GA showed ascendant specific adsorption capacity (SAC) of 16 mg/g at 1.2 V, revealing a high CE of 62.5 %, and attained 83.2 % capacity retention of 80 adsorption–desorption cycles at 0.8 V. As CS + 3GA conveyed more positive charges and had high hydrophilicity. Moreover, a freestanding chitosan-based porous carbon nanofiber (PCNF) electrode was fabricated without any binders or additives to avoid the negative impact of the additives on the electrochemical performance [118]. The fabricated electrode possessed a BET SA of 700 m^2/g and a hierarchical pore structure. The chitosan-based PCNF exhibited a high SAC of 23.6 mg/g and charge efficiency of 85 %. Chitosan-boric acid hydrogel was fabricated using magmatic stirring followed by freeze-drying [119]. The produced gel was then carbonized at 800 °C under nitrogen to obtain boron-nitrogen-doped carbon nanosheets (BNC). The BNC was decorated with manganese oxide under different reaction times (2, 4, and 6 h) to obtain MnO-2@BNC, MnO-4@BNC or MnO-6@BNC. The different MnO-t@BNC were investigated as cathode electrodes in CDI cells for water desalination. Among different electrodes, MnO-4@BNC achieved a desalination amount of 20.3 mg/g and a specific capacitance of 249 F/g. the synergistic effect of MnO_2 and BNC improved the performance of the CDI system.

3.4. Industrial waste-based electrode materials

This section summarizes the progress done in fabricating activated carbon from various industrial wastes for CDI electrodes.

Polystyrene foam: Recent developments in plastic production and waste management predict that by 2050, nearly 12,000 Mt of plastic and other non-biodegradable waste will be accumulated in landfills and the natural environment [120]. Expanded polystyrene (EPS) foam waste was used as raw material to produce a hyper-crosslinked polymer, which acted as a scaffold to produce a new *N*-doped porous carbon. The resulting material showed a SSA of 810 m^2/g, a total pore volume of 0.8 cm^3/g, a specific capacitance of 327 F/g, and a 100 % capacitance retention after 10,000 cycles of charge/discharge. Furthermore, a strong electrosorption capacity of 34.8 mg/g at 1.6 V using 500 mg/L NaCl sol. was obtained [121].

Glucose and glucosamine: The CDI performance using nanoporous heteroatom-doped carbon derived from glucose and glucosamine using a refined salt templating approach was investigated [122]. The *N*-doped carbon activated with cesium

acetate at 900 °C displayed a SSA of 2830 m^2/g, a pore volume of 1.56 cm^3/g, a specific capacitance of 132 F/g, and a salt adsorption capacity of 15.0 mg/g at 1.2 V in 5 mM aqueous NaCl. However, the electrode had a relatively low charge efficiency of 0.64; this can be linked to the high heteroatomic content, which affects the material's surface chemistry. Microporous carbon spheres (CSs) produced from glucose by carbonization at different temperatures (Fig. 7 (a)) were investigated as electrode materials for CDI cells. Results showed that the SSA was increased from 271.5 m^2/g to 361.1 m^2/g by increasing the carbonization temperature from 700 to 800 °C, linked to complete sample carbonization. Further increase of the carbonization temperature to 900 °C resulted in a decrease in the SSA to 211.7 m^2/g) as a consequence of sintering and pore structural damage. CS800 exhibited the highest capacitance of 71 F/g at a scan rate of 5 mV/s, a high electrosorption capacity of 10.3 mg/g at 1.6 V (Fig. 7 (b)), and a complete regeneration after 20 ads/des cycles [123].

Polyaniline: Precursors that contain nitrogen compounds such as glucosamine hydrochloride [124], polyacrylonitrile [125], polyaniline (PAni) [126], and polypyrrole [127] have been a low-cost alternative for obtaining post-treatment *N*-doped AC. Activated carbons were developed using PAni as *N*-containing precursor, then doped with varying anions and investigated in the CDI [128]. The impact of polystyrene sulfonate (PSS), chloride (Cl), dodecylbenzene-sulfonate (DBS), and p-toluenesulfonate (PTS) as doping agents on the PAni activate carbon (PAC) performance as an electrode was investigated. The highest capacitance at 1.0 mV/s of 90 F/g was obtained for the PAC/PTS electrode, followed by PAC/DBS (89 F/g), and PAC/PSS (88 F/g). PAC/PTS also exhibited the highest electrosorption performance of 14.3 mg/g at 1.2 V, the highest charge efficiency (81–90 %), and the lowest energy consumption (3.8–4.2 kJ/g).

Novolac: Novolac is an industrial polymer that is produced in large quantities as a byproduct of several industries. Novolac can be used to obtain sub-micrometre sized nanoporous carbon beads to act as electrodes for CDI. The polymer beads were fabricated through a self-emulsifying system, then pyrolysis and CO_2 activation. The resulting material showed a SSA of 1905 m^2/g, a total pore volume of 1.26 cm^3/g, and a specific capacitance of 124 F/g at a specific current of 0.1 A/g. CDI tests performed at 1.2 V in 5 mM NaCl exhibited a salt sorption capacity of 8 mg/g. A salt adsorption capacity of 11.5 mg/g was achieved after electrode treatment with hydrogen; this treatment showed 80 % charge efficiency and higher stability (90 % after 100 cycles). Although the H_2 treated electrode's salt adsorption capacity is similar to other high-performance commercial AC materials, the average deionization rate of 0.104 mg/g/s is far higher, surpassing commercial activated carbons [129].

3.5. Summary and discussion

Various biomass resources were used to fabricate carbon electrodes for CDI systems. Table 1 summarizes the progress of implementing bio-based electrodes in the CDI for water desalination. It can be observed from the table that most of the work focuses on plant-based precursors, such as rice plants, cotton, bamboo, and coconut, while much fewer works used animal-based and industrial-based electrodes. Therefore, considerable work can be done to consider these two types of wastes, especially they have

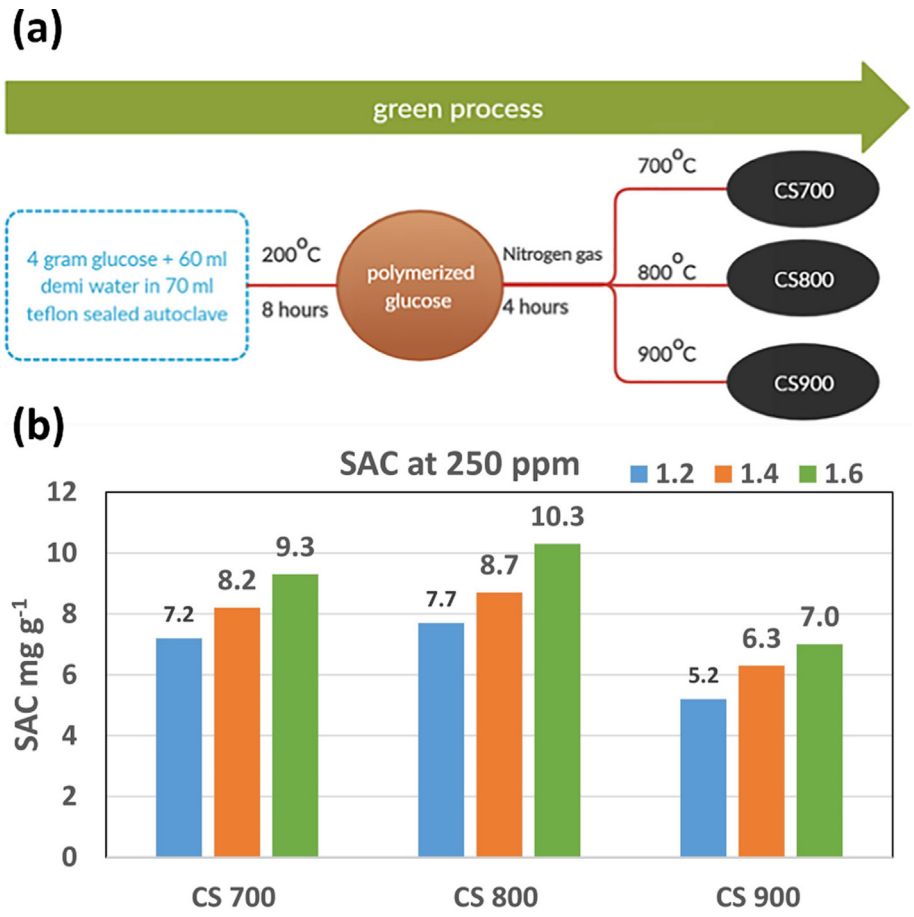

Fig. 7. (a) Fabrication process of microporous carbon using glucose as a precursor, (b) SAC of the three produced electrodes at an initial concentration of 250 ppm adapted from [123], with permission No. 5414291339389.

Table 1
Progress on implementing biomass and waste-based electrodes in desalination by capacitive deionization systems.

Type	Resource	Type of Carbon Electrode	Type of operation	Specific surface area (m2/g)	Specific capacitance (F/g)	Scan rate (mV/s)	Current density (A/g)	Salt removal percentage (%)	Initial cond. (µS/cm)	Initial conc. (mg/L)	Voltage (V)	Salt adsorption capacity (mg/g)	Average Salt adsorption rate (mg/g/s)	Charge eff. (%)	Ref.
Plant-based	Cotton	carbon sponge	Batch	2680	109.9	10				500	1.2	16.1		77	[79]
	Sugarcane	Biochar	Batch	1019	208	5				292	1.2	28.9			[80]
	Rice plant	Biochar	Single pass	1839	120.5	5				116	1.2	8.11	0.0153	48	[85]
	Shiitake mushrooms	AC	Batch		247.6	1			1050		1.2	12.9			[89]
	Sugarcane fly ash	AC	Batch	350	55	1			1250	600	1.2	5.3			[139]
	Soybean shell	*N*-doped porous carbons	Batch	1036.2	215.3		0.25		82.3	40	1.2	15.5	0.0148		[46]
	Bamboo/MnO_2	AC	Batch	1747	158.2	10				105	1.2	10.3			[91]
	date palm/ MnO_2	AC	Batch	1224	259	10			1200	600	1.2	17.8		55	[92]
	Loofa sponge	AC	Batch	1819	93	5		>90	1025	29.2	1	22.5			[104]
	Lotus leaf	Carbon Nanosheets	Batch	4482	289		0.5		1085	2000	1.6	65			[98]
	Peanut shell/ MnS_2	AC	Batch	13.34	113	10		35	2050	1000	1.2	8.89			[103]
	Almond shell	AC	Batch	452						500	1.2	19.2			[49]
	Pinecones	P-doped porous carbon	Batch	1176	238	5			970	500	1.2	14.62			[132]
	Pine	Porous carbon	Batch	1016	94.16	10			500		2	19.43		42	[102]
	Coconut shell	AC / CNT	Batch	630	90.2	20			522	200	1	14.1			[106]
	Tamarind shell	AC	Batch	410	174.5	10			1280	600	1.2	18.8		83	[109]
	Jackfruit	AC	Batch	1955	307	5		95	72.2	30	2	1.18			[110]
	Date seeds	AC	Batch	1020.85	400	10			512	250	1.2	22.2		86	[96]
	Citrus peel/$ZnCl_2$	AC	Batch	323	120	1			1050	500	1.5	16	0.0167	61	[111]
	Watermelon/ $MnFe_2O_4$	AC	Batch	483	425	10			510	250	1.2	29		96	[112]
	Coconut shell/MnO_2	AC	Batch	304	410	5		83.4		1000	1.2	68.4		24	[107]
Animal-based	Egg white	*N*-doped porous carbons	Batch	3277.96	136.61	100				500	1.2	26.67			[113]
	Leather wastes	Carbon Aerogel	Batch	2523	132.2	2				500	1.2	20.29			[114]
Industrial waste-based	Chitosan	AC	Batch	2727						500	1.2	14.12	0.00567		[116]
	Glucose and Glucosamine	Heteroatom Doped Carbons	Single-pass	2830	132					292	1.2	15		64	[122]
	Polystyrene foam	*N*-doped porous carbons	Batch	810	327		1			500	1.6	34.8			[120]
	Glucose	carbon spheres	Batch	361.1	71	5			200	250	1.6	10.3			[123]
	Thermoplastics	Carbon Aerogel	Single-pass	1785	173		0.5	99.73		50	1.2				[140]
	Novolac	carbon beads	Single-pass	1905	124		0.1			29.2	1.2	11.5	0.104	40	[129]
	polyaniline	AC	Batch	1484	90	1				600	1.4	14.9	0.033	90	[128]

already been applied in several applications and proved efficient [130,131]. By looking at the current progress, it can be observed that the best performing electrodes were those doped with heteroatoms, such as nitrogen or phosphorus [46,132], or those formed composites with metal nanoparticles, such as MnO_2 [91,107] and $MnFe_2O_4$ [112]. These results prove the effectiveness of heteroatom doping and forming composites with metal nanoparticles in increasing the performance of biomass/waste-based electrodes. However, other types of heteroatoms that proved their usefulness, such as boron [133] and sulfur [134], should be tested with bio-based carbon electrode materials. The co-doped carbon materials in which two types of heteroatoms are added together to the carbon electrode [135] is also a promising process to enhance the electrode's performance. Other types of nanoparticles should be investigated with biomass/waste-based carbon materials, such as TiO_2 [30], CeO_2 [136], MoS_2 [137], and ZnO [138]. Investigating these types of composites can significantly increase the performance and applicability of biomass and waste-based electrodes in CDI applications.

4. Use of bio-based electrodes in CDI for wastewater treatment

Another important application of CDI systems is wastewater treatment. Due to industrial and population growth in many countries worldwide, the amount of wastewater produced from the industrial and domestic sectors increases yearly. Given this situation, it is important to establish feasible and effective wastewater treatment technologies. CDI arises as a potentially cheap and effective alternative to current wastewater treatment technologies such as reverse osmosis [141,142] and nanofiltration [143]; as well as other emerging technologies such as microbial fuel cells [144–148]. Using abundant and cost-effective carbon precursors for producing CDI carbon electrodes will make the technology more attractive. This section summarises and discusses the application of bio-based electrodes in CDI systems for wastewater treatment.

4.1. Heavy metal ions removal

The presence of heavy metal ions in wastewater resulted in severe health and environmental effects. For example, increased amounts of lead in drinking water may result in kidney problems, muscle and joint pains; while elevated amounts of chromium can cause lung tumors [149 150]. Heavy metal ions include chromium, copper, nickel, lead, arsenic, zinc, mercury, and cadmium. The removal of such heavy metal ions is essential from the health and environmental point of view. This section summarises the progress in using bio-based CDI cells' for the removal of heavy metal ions.

4.1.1. Chromium

Peanut shell: Activated carbon derived from peanut shell (PSAC) (Fig. 8 (a)) and its iron oxide composite (Fe_3O_4/PSAC) were produced and examined as a potential CDI electrode for chromium ions' removal from wastewater (Fig. 8 (b)). Fe_3O_4/PSAC composite had higher Cr(VI) removal efficiency compared to pure PSAC. Even though the smaller SSA of Fe_3O_4/PSAC (525 m^2/g) compared with PSAC (751 m^2/g), the composite adsorbent showed better adsorption and recyclability owing to Fe_3O_4 magnetic activity (Fig. 8 (c)). Moreover, BET and Fe_3O_4/PSAC electrochemical analysis proved its mesoporous structure and high pseudo-capacitance of 610 F/g (10 mV/s), with good stability and reduced internal resistance. CDI removal applications using Fe_3O_4/PSAC showed total removal of Cr(VI) of 9.9 % with an excellent electrosorption capacity of 24.5 mg/g at pH 6.5, as shown in Fig. 8 (d) [151].

Tea waste: Microporous activated carbon was developed by thermal and chemical modification of tea waste biomass (TWBAC) to be used as electrode material in CDI for chromium ions' removal and F removal [152]. The electrode was observed to have a peak electrosorption capacity for F and Cr(VI) of 0.74 and 0.77 mg/g at 10 mg/L and 2.49 and 2.83 mg/g at 100 mg/L, respectively. After simultaneous electrosorption of Cr(VI) and F, the TWBAC electrode was successfully regenerated. Compared to monovalent F-, the electrosorption selectivity of the divalent chromate allowed a higher removal of chromium ions.

Rice husk: Acid-activated carbon from rice husk was employed as a carbon precursor for electrodes to be used in capacitive deionization. The sulphuric acid-treated rice husk waste activated carbon (RHWBAC) used for the removal of Cr(VI) displayed an electrosorption capacity of 2.83 mg/g at 100 mg/L feed concentration at 1.2 V. The maximum Cr(VI) removal for 10 mg/L feed concentration was reported to be 85 %. The results indicated that the electrosorption process fits the Langmuir isotherm model, Redlich Peterson isotherm, and the Pseudo kinetic first-order model. Besides, the computational fluid dynamics (CFD) analysis of the square CDI layout reveals that the stagnant regions decrease with increasing feed flow rates. Furthermore, following Cr(VI) sorption, the RHWBAC electrode's successful regeneration was recorded [153].

Corncob waste: A porous carbon with a 3D honeycomb-like composition (3DHPC) was fabricated from corncob waste by hydrothermal carbonization combined with KOH activation for chromium removal using a CDI system [154]. The electrode showed a hierarchical mesoporous and macroporous structure, a SSA of 952 m^2/g, a specific capacity of 452 F/g, and a removal efficiency of 91.58 % at 1.0 V using 30 mg/L Cr(VI) solution. Chromium removal efficiency was considerably increased to 96.20 % at an applied voltage of 2.0 V. The improved adsorption arises from the affinity between chromium (VI) ions and the electrode.

Red oak: Red oak bio charcoal, a relatively cheap and very conductive electrode material, was used for chlorine and chromium extraction from leather treatment wastewater. Biocharcoal treated with KOH resulted in an adsorption capacity of 13.79 mg/g and a specific surface area of 303.59 m^2/g; compared to charcoal treated with Fe_2O_3, these values represent an increment of 40 % and 80 %, respectively. After 10 cycles of the CDI system operation, the removal rates of Cl^- and Cr^{3+} in leather processing wastewater approached 86 % and 100 %, respectively. The KOH-activated electrodes resulted in good regeneration performance after 2.5 cycles; however, the adsorption capacity decreased from 10.77 to 10.57 mg/g after regeneration [48]. The electrode obtained could potentially replace other electrodes for removing chlorine and chromium ions.

Bael fruit: AC from Bael fruit shell was used to form a biocomposite with polyvinyl alcohol (PVA) in a ratio of 1:4 for the removal of Cr (VI) ions. PVA is a synthetic organic material consisting of a non-crystalline polymer with biodegradable nature and excellent electrical conductivity features. The synthesized AC layer has a mesoporous and macroporous composition with a large SSA of 617.72 m^2/g. It also showed a high adsorption capacity of 294.5 mg/g and 100 % removal efficiency at 15 V [155]. The biocomposite electrode could be remarkably used for wastewater treatment owing to its suitable biodegradability and electrical conductivity.

4.1.2. Lead

Chicken feather: Porous carbons from chicken feathers (CF) was synthesized and chemically activated by KOH under a nitrogen stream for 3 h [76]. The developed materials were employed to eliminate lead from a lead (II) nitrate solution in a CDI cell. The

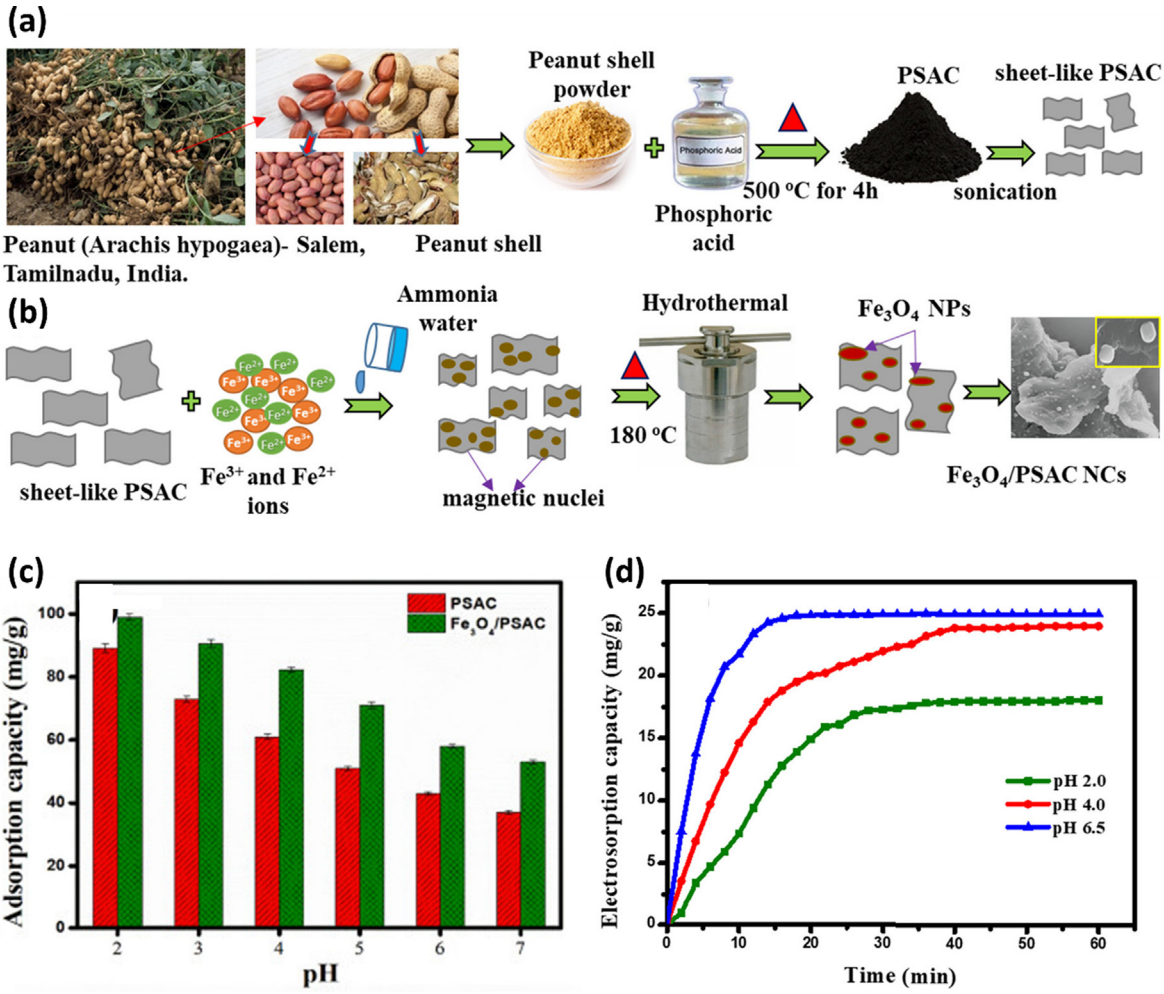

Fig. 8. (a) Synthesis process of peanut shell activated carbon (PSAC) using pyrolysis, (b) Synthesis of Fe_3O_4/PSAC nanocomposites using a hydrothermal treatment, (c) Adsorption capacity of both electrode materials under different pH values and a concentration of 50 mg/l, (d) Electrosorption capacity of the Fe_3O_4/PSAC nanocomposites electrode at 1.2 V and 50 mg/l, adapted from [151], with permission No. 5414300049446.

untreated carbon surface area was estimated to be 642 m^2/g which increased to 1642 m^2/g after KOH activation at 800 °C. The lead removal test conducted using a CDI cell, including the manufactured carbon electrode and 100 mg/L $Pb(NO3)_2$ solution showed a removal percentage of 81 % and an electrosorption capacity of 4.1 mg/g at (applied potential of 1.2 V and a flow rate of 5 mL/min).

4.1.3. Arsenic

Thermoplastic waste: A novel, non-invasive, and chemical-free approach was proposed to manufacture highly porous carbon aerogels from thermoplastic waste by eliminating the current sol–gel method's drawbacks. The new method involves three steps: (1) hydrothermal carbonization, (2) freeze-drying, and (3) post-pyrolysis; the produced material was immobilized on a locally accessible, biocompatible, and flexible jute thread substrate. The specific surface area of ACs was 1785 m^2/g with a specific capacitance of 173 F/g at 0.5 A/g. Moreover, without applying any voltage, the electrode was still able to extract salt and heavy metal pollutants from the feedstock solution, and complete removal was achieved after applying an additional voltage of 1.2 V. Using concentrations below 1000 mg/l, the cell achieved a high arsenic removal percentage of 99.79 % that decreased to 95.21 % at higher concentrations up to 2000 mg/l [140].

4.1.4. Other heavy metal ions:

Polyvinyl chloride plastic waste: S, *N-co*-doped carbon materials (sN-C) was developed from polyvinyl chloride (PVC) plastic waste and examined as CDI electrode for removing heavy metals ions (Cd^{2+}, Ni^{2+}, Co^{2+}, Pb^{2+}, $Fe^{2+,}$ and Cu^{2+}) [156]. For a heteroatom concentration of 13.30 % S and 4.55 % N, the SSA was 1230 m^2/g, the capacitance was 290.2 F/g (at 1.0 A/g), the removal efficiency was 94–99 %, and the capacity was 36–62 mg/g (Fig. 9). Experiments revealed the sN-C electrode's high efficiency and impressive stability throughout five consecutive adsorption/desorption cycles.

4.2. Nutrients removal

In many cases, plant nutrients can be found in considerable amounts in wastewater. These nutrients include ions that contain nitrogen, phosphorus, and potassium, such as nitrite (NO_2^-) [157], nitrate (NO_3^-) [158], and phosphate (PO_4^{3-}) [159]. Bacterial cellulose (BC) is an available, inexpensive, and sustainable resource, and carbonized bacterial cellulose (CBC) is an excellent base material for carbon electrodes. CBC-based electrodes coated with proportions of sulfosuccinate acid (SA) and glutaric acid (GA) were developed for nitrate removal in CDI cells. The specific capacitances of CBC-GA and CBC-SA were 124.23 and 169.41 F/g. CBC-SA electrode displayed the highest salt adsorption capacity of 14.56 mg/g and

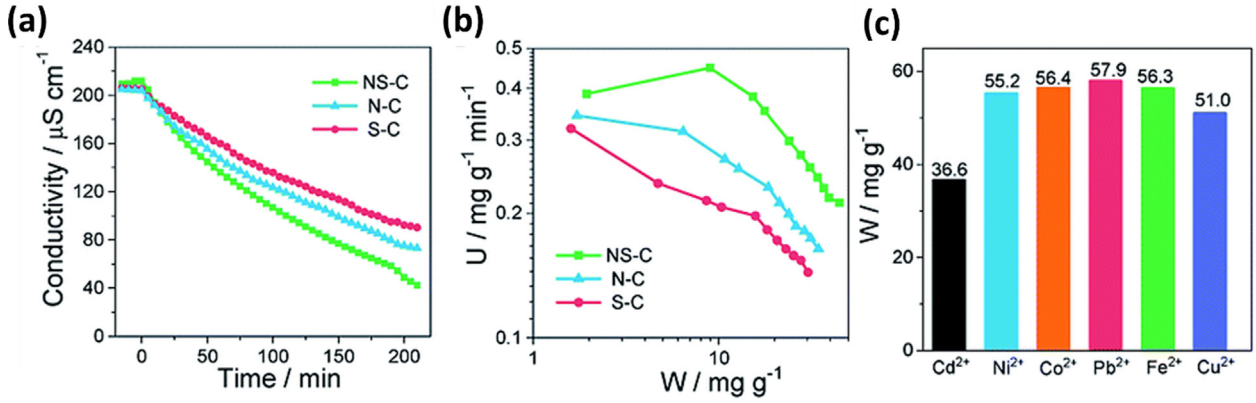

Fig. 9. (a) The electrosorption experiment at 1.5 V and 50 mg/l and (b) the CDI Ragone plot of the three synthesized electrode materials in Fe^{2+} solution, (c) The SAC obtained for each of the six heavy metal ions using NS-C electrode [156], open access.

Table 2
Summary of the application of biomass/waste-derived electrodes in wastewater treatment CDI systems.

Type	Removed ion	Electrode material	Applied voltage (V)	Initial ion concentration (mg/L)	Removal percentage %	Salt adsorption capacity (mg/g)	Reference
Heavy metal	Cr(VI)	Peanut Shell/Fe_3O_4 (Fe_3O_4/PSAC)	1.2	200	99.9	24.5	[151]
	Cr(VI)	Rice Husk (RHWBAC)	1.2	100	85	2.8316	[153]
	Cr(VI)	Corncob (Porous carbon)	2	30	96.2		[154]
	Cr(VI)	Bael Fruit (AC)	1.5	10	100	294.5 (using methylene blue number)	[155]
	Cr(VI) / F	Tea Waste (AC)	1.2	10	88.5 / 85.2	0.77 / 0.74	[152]
	Cr(III)/ Cl	Red Oak (bio charcoal)	1.2	2.03 / 4665.2	86.7 / 100	13.79 (for both ions together)	[161]
	Pb^{2+}	Chicken feathers (Porous carbon)	1.2	100	81	4.1	[76]
	Fe, Co, Ni, Cu, Pb, Cd	Polyvinyl chloride plastic (sN-C)	1.5	50	94–99	56.3/56.4/55.2/51.0/57.9/ 36.6	[156]
Nutrient	NO_2^-	Bacterial cellulose (CBC)	0.8–1.2	24.54	71	14.56	[160]

71.01 % nitrate removal efficiency. Increasing the applied voltage from 0.8 to 1.2 V resulted in increasing the adsorbed anions. The findings showed that the polymer coating resulted in an excellent total ion removal efficiency and improved the nitrite's removal [160].

4.3. Summary and discussion

Several studies investigated the use of bio-based CDI electrodes for wastewater treatment, as seen in Table 2. It is clear from the table that doping the bio-based carbon electrodes with the transition metals such as Fe_3O_4 significant improved their adsorption capacity [151]. The same behaviour is noticed in the case of heteroatoms [156]. It can be observed from the table that most works focused on the removal of heavy metals from wastewater, and most of these works investigated the removal of chromium ions yielding removal percentages higher than 80 %. Despite the importance of chromium removal, further investigations for the removal of other heavy metal ions, such as mercury, nickel, copper, and cadmium, are still needed. Furthermore, few studies focused on removing nutrients from wastewater, therefore, more work should be done to investigate the suitability of waste-based electrodes for this application. Other types of contaminants that can be studied include ammonia, nitrate, phosphate, and lithium.

The main finding of the application of the Biobased CDI electrodes in the desalination (salt adsorption capacity) and wastewater treatment (Cr ion removal) can be summarized in Fig. 10. As being clear from the figure that the different biobased activated carbon materials demonstrated a high salt adsorption capacity that reached more than 25 %, Fig. 10a, and an excellent removal of the Cr ions from the wastewater that reached 100 %, Fig. 10b.

5. Promising bio-based electrodes for CDI

Due to the high similarity in the operation mechanism between CDI cells and supercapacitors, the same electrode materials can be used in both applications. Several studies focused on bio-based supercapacitor electrode materials, which are considered promising candidates for CDI applications. MnO_3Si hybridized carbon's electrode derived from natural bamboo leaves was used in supercapacitors [162]. The electrode's capacitance was 162.2F/g and the specific surface area was 300.3 m^2/g. After 10,000 charge/discharge cycles, 85 % capacitance retention was recorded. Porous AC micro sheets from pomelo seeds were developed and investigated in supercapacitors [163]. The pomelo seeds-based AC electrode exhibited a specific capacitance of 240 F/g and a specific surface area of 807.7 m^2/g with a 100 % capacitance retention after 10,000 cycles. Similarly, a pomelo peel-derived carbon was prepared by activation with N and Co in one-pot pyrolysis [164]. The electrode exhibited high surface area, high specific capacitance (325 F/g), and excellent cycling stability, making it a promising electrode for CDI application. Using the same material, Yang et al. [165] reported for the first time the production of tri-modal porous carbon with an outstanding capacitance of 550 F/g at 0.2

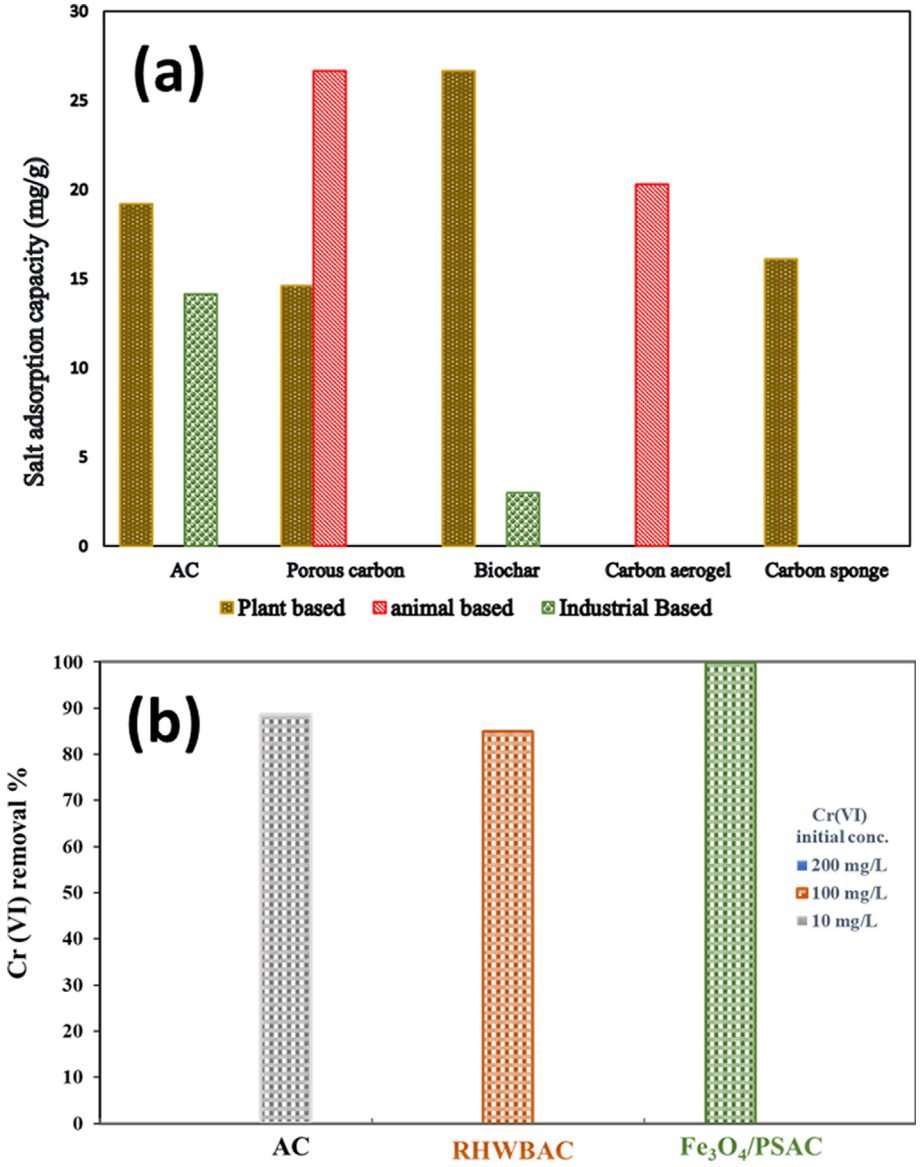

Fig. 10. (a) Salt adsorption capacity of different biobased carbon CDI electrodes at 1.2 V and 500 mg/L NaCl, and (b) Cr removal using biobased CDI electrodes, i.e., activated carbon (AC), sulphuric acid-treated rice husk waste activated carbon (RHWBAC), and activated carbon derived from peanut shell and iron oxide composite (Fe_3O_4/PSAC).

A/g for biochar obtained from pomelo endothelium (prepared by metal ion impregnation and molten KOH activation). The resulting SSA was 1265 m^2/g; the material showed a hierarchical porous structure and high graphitization level. Hierarchical nano-micro porous carbon spheres prepared using composites derived from rice straw exhibited a SSA of 1122 m^2/g with a specific capacitance of 337 F/g [166]. Simple chemical activation synthesized a novel hierarchical carbon with a high surface area (2742 m^2/g) from cashew nut husk biomass [167]. The sample exhibited a superior capacitive performance (305.2 F/g) and 97.1 % capacity retention after 4000 charge–discharge cycles. Biochar electrodes derived from *Cladophora glomerata* macroalgae were fabricated with well-ordered micro/macro porous structure and have high carbon content [168]. The electrode displayed SSA of 354 m^2/g with a specific capacitance of 376.7 F/g, as well as strong stability showing only a 0.8 % reduction in capacitance after 5000 cycles. In a similar work, novel biochar interconnected 3D pore structure electrode derived from *Cladophora glomerata* macroalgae was synthesized [169]. The obtained electrode displayed SSA of 957 m^2/g and a specific capacitance of 418 F/g, along with a stable cycling performance of 93.1 % after 10,000 cycles. A novel algae-derived nitrogen-containing porous carbon was developed and used as electrode material [170]. The porous carbon has a very high SSA of 1538.7 m^2/g and a specific capacitance of 287.7 F/g with cycling stability of 98 % capacitance retention after 8000 cycles. In other study, a hierarchical porous CO_2-activated carbon aerogel was prepared from cellulose with desirable macropores, mesopores, and micropores [171]. The aerogel had SSA of 1364 m^2/g and a specific capacitance of 328 F/g, and well stability of 96 % capacitance retention after 5000 charge/discharge cycles. A hierarchical porous carbons with high SSA and total pore volumes were produced using a sustainable one-pot structure based on products from biomass [172]. The methodology involved thermal treatment of biomass (glucose, glucosamine, soy flour, and microalgae) using a soft activating agent (potassium oxalate) and a hard substrate (calcium carbonate nanoparticles). The materials fabricated at 800 °C have large SSA within a range of 1800–3100 m^2/g. Huang et al. [173] produced a hierarchical porous carbon using waste animal bones and evaluated its performance as a supercapacitor electrode. The material demonstrated SSA of 2157 m^2/g which led to a good speci-

Table 3
Promising biomass/waste-based electrodes for the application in CDI.

Resource type	Resource	Carbon material	Specific Surface Area (m^2/g)	Specific Capacitance (F/g)	Current density (A/g)	Reference
Plant-based	Bamboo leaves	Manganese silicate hybridized carbon	300.3	162.2	0.5	[162]
	Rice straw	Carbon Spheres	1122.0	337.0	1.0	[166]
	Green tea waste	Graphitic carbon nanoflakes	1057.8	162.0	0.5	[174]
	Silk	Microporous Carbon Nanoplates	2557.0	264.0	0.1	[175]
	Wood	Activated carbon fibers	3223.0	247.0	0.5	[176]
	Cashew nut	Hierarchical porous carbon	2742.0	305.2	1.0	[167]
	Pomelo peels	Activated Carbon	807.7	240.0	0.5	[163]
	Pomelo peels	Activated Carbon	–	325.0	1.0	[164]
	Pomelo endotheliums	Carbon Biochar	1265.0	550.0	0.2	[165]
	Baobab fruit shells	Activated Carbon	911.7	355.8	1.0	[177]
	Banana fibers	Activated Carbon	1097.0	74.0	0.5	[178]
	Apple-ring acacia fruit	MnO2/Carbon spheres	525.1	426.0	1.0	[179]
Animal-based	Cow dung	Activated Carbon	1984.0	124.0	0.1	[180]
	Animal bone	Hierarchical porous carbon	2157.0	185.0	0.05	[173]
Waste-based	*Cladophora glomerata* macroalgae	Carbon Biochar	354.0	376.7	1.0	[168]
	Cladophora glomerata macroalgae	Carbon Biochar	957.0	418.0	1.0	[169]
	N. Salina Algae	Porous Carbon	1538.7	287.7	0.2	[170]
	Human hair	Porous carbon flakes	1306.0	340.0	1.0	[130]
	Cellulose	Carbon Aerogels	1364.0	328.0	0.5	[171]

fic capacitance value of 185 F/g at 0.05 A/g. Table 3 summarizes some of biomass and waste-based supercapacitors electrodes performance. These electrodes are promising candidates for high-performance CDI systems.

6. Comparison between bio-based electrodes and commercial ones

Carbon electrodes produced from bio-based materials display good potential as a low-cost alternative to relatively expensive conventional carbon nanomaterials, such as CNTs, CNFs, and graphene. However, this cheaper alternative may show lower performance due to the non-defined structures. This section compares bio-based electrodes and conventional carbon electrodes based on resource availability, ease of manufacture, cost, material specification, and performance.

6.1. Resource availability

The availability of the carbon precursor is a significant factor that must be considered in the CDI systems. A more available source means a cheaper source as well. Activated carbon is currently the most used CDI material due to its high porosity, high surface area, and high adsorption capacity. In general, activated carbon derived from natural or biomass sources, such as coconut shells, tea leaves, and wood, is widely available worldwide [181]. The carbonization of synthetic polymers can also derive AC; however, these polymers have many different applications other than electrode fabrication, impacting their availability. The availability of an electrode material with high salt adsorption capacity is one of the main challenges that restrict CDI technology's scaling up [182]. The massive availability of carbon materials extracted from biomass residues can produce CDI electrodes with high electrosorption capacity. On the other hand, synthetic carbon nanomaterials show a lower availability than bio-derived materials, reflecting the commercial price.

6.2. Ease of manufacture

AC powder is primarily synthesized through pyrolysis of carbon source materials such as wood and nutshells below 1000 °C. The source carbon materials are initially pyrolyzed below 800 °C, and then activated between 950 and 1000 °C. Chemical activation also can be carried out using a salt, an acid, or an alkali and then carbonized at temperatures between 400 and 700 °C [183]. Carbon aerogel fabrication is more complex, starting with the sol–gel polymerization of resorcinol with formaldehyde creating cross-linked hydrogels that are dried out to form the precursor aerogel. The aerogel is subjected to pyrolysis at high temperatures, producing the final carbon product [184]. Carbon nanotube fabrication methods include chemical vapor deposition, arc discharge, high-pressure CO disproportionation, and laser ablation. Most of these procedures are expensive as they occur under vacuum conditions [185]. On the other hand, biobased activated carbon can be produced using ease and simple methods compared with the aforementioned methods that proved the feasibility of activated carbon from biomass sources as a CDI electrode material [45,46].

6.3. Cost

Previous studies proved that high-performance AC could be obtained from wastes like coconut shell [106], peanut shell [103], or almond shell [49], and other biomass materials with minimum or negligible cost. Moreover, activated carbon can be obtained from animal waste such as eggshells [113], animal hairs [186], or animal bones [131]. March and Reinoso [187] stated that bio-based derived carbon could be available at a cost of 0.50 €/kg. On the other hand, petroleum residues, coal, lignite, peat, and polymers used as precursors for conventional production of AC, are more expensive and nonrenewable [188], while graphene powder cost ranges between 50-$200/kg, depending on the quality and volume.

6.4. Material specification

The electrode material's surface characteristics, such as the SSA, pore size distribution, pore structure, and surface functional groups, affect the electrodes' electrosorption capacity [189]. Studies reported that bio-based carbons display high specific surface area, good electrical conductivity, controlled pore architecture, and allow high specific capacitance values [111,190]. Additionally, doped carbon materials derived from biomass have acquired extensive CDI applications due to their smaller ion transfer and

higher surface area, ensuring a high specific capacitance and ionization capacity [191–193]. Sometimes, high electrical resistance and low capacitance are found in biomass-derived electrodes. Pore structure modification or combined oxygenated groups addition are among the strategies used to solve this major drawbacks [194,195]. Some studies have revealed that graphene can reach a theoretical SSA of 2630 m^2/g, a much greater value than the 900 m^2/g for carbon black or the 1315 m^2/g for carbon nanotubes [196,197]. Although graphene is an excellent adsorbent, it can agglomerate in the redox process, decreasing its SSA and dramatically influencing the conductivity and the ion transfer rate [198,199]. Carbon nanotubes are also considered strong applicants for CDI, owing to their high aspect ratio, high surface area, and extraordinary thermal, electrical, and mechanical properties [200,201]. It is reported that the specific capacitance of carbon nanotubes is lower than that of activated carbon, but their conductivity is higher [57]. Furthermore, carbon aerogel achieves excellent properties, but its progress is limited due to its high cost and complicated production process.

6.5. Performance

As previously stated, AC is currently the most widely used material for CDI, given its high porosity, facilitating the absorption of ions and water-polluting species. The highest salt absorption capacities were achieved using biobased activated carbons extracted from Loofa sponge, watermelon peel, and cotton waste, resulting in 22.5 mg/g [104], 17.38 mg/g [202], and 16.1 mg/g [79], respectively. These values are comparable and even higher in some cases than the corresponding from conventional electrode materials such as graphene (22.27 mg/g) [203], carbon nanotubes sponge (4.3 mg/g) [204], and carbon aerogels activated by CO_2 (8.4 mg/g) [205]. Although carbon materials generally prove their excellent properties in many applications, including electrode manufacturing, their synthesis and cost play a crucial role in the market. Activated carbon is cheap, easy to obtain, and possesses most of the required CDI applications' required properties, making it the most used material for CDI electrodes. Table 4 shows a performance comparison between biobased carbon electrodes and some conventional carbon nanomaterials as CDI electrodes.

6.6. Summary and discussion

Bio-based derived carbon features wide resource availability, ease of fabrication, scalable, and cheap. However, these materials need nano-scale modifications to overcome their poor performance. On the other hand, conventional carbon nanomaterials have a lower resource availability, harder fabrication, and higher production cost. Still, in return, they show better material specifications and overall better capacitive performance. These results show the cost-performance tradeoff, which should be considered when choosing a CDI system (Table 5).

7. Recommendation and future prespectives

Despite the increasing number of publications on the development of bio-based carbon electrodes for CDI applications, there

Table 4
Comparison between the performance of biomass/waste-based electrode materials and conventional electrode materials in CDI systems.

Type	biomass	Specific surface area (m^2/g)	Scan rate (mV/s)	Specific capacitance (F/g)	Initial salt concentration (mg/L)	Voltage (V)	SAC (mg/g)	Ref.
Biomass/waste-derived electrodes	Pomelo peel *meso*/microporous carbon	2726	1	207.0	1000	1.4	20.78	[192]
	Wasted coffee grounds *meso*/microporous carbon	1856	10	180.3	292	1.4	16.50	[206]
	Coconut shells mesoporous AC	1040	–	–	50	1.6	3.75	[207]
	Raw cotton carbon sponge	2680	10	109.9	500	1.2	16.10	[79]
	Woody biomass activated biochar	1675	0.5	240.0	500	1.2	5.39	[208]
	Soybean shell *N*-doped porous carbon	1036	2	165.0	1000	1.2	43.3	[46]
	Watermelon peel *meso*/microporous carbon sheets	2360	1	224.0	500	1.4	17.38	[202]
	Polystelyne foam *N*-doped porous carbon	810		327	500	1.6	34.8	[121]
Conventional electrode materials	3D Graphene	124		219.6	572	2.0	29.6	[209]
	Ordered mesoporous carbons	844	1	133	25	1.2	0.68	[210]
	Carbon aerogels	400–1100				1.2	3.33	[211]
	Carbon nanotube	153			3500	1.2	9.35	[212]
	Carbon nanofiber	186	10	222.3		1.2	1.91	[189]
	Carbon nanospheres	1321	1	243	500	1.6	5.81	[213]
	Reduced graphene oxide	137.4		112	40	2.0	1.51	[214]

Table 5
A general comparison between bio-based carbon and conventional carbon nanomaterials.

Criteria (worst 1–5 best)	Biomass/waste-based carbon	Conventional carbon nanomaterials
Resource availability	Widely available (5)	Less availability (4)
Ease of fabrication	Easy fabrication, suitable for large-scale production (5)	Harder fabrication, challenging to large-scale produce (3)
Cost	Cheap (5)	Generally more expensive (2)
Material specifications (Surface area, porosity)	Good specifications, but needs modifications (3)	Great specifications (4)
Performance	High performance (4)	Excellent performance (5)

are still many research topics that worth investigating to deepen the practical application of such materials. These topics include:

- No pilot-scale CDI systems using bio-based carbon electrodes tested. Research on CDI bio-based carbon electrodes will stay far from the large-scale application if no real demonstrations of its operational performance are available.
- Performing a long-term economic analysis of bio-based CDI systems and comparing it with those using conventional carbon electrodes is essential to give a deeper insight into the performance-cost tradeoff of such systems.
- Although massive work has been done on investigating the effect of doping biobased carbon materials with heteroatoms on the performance of supercapacitors [215–217], few works have been done on CDI [109]. Therefore, it is recommended to investigate such an effect on the performance of the CDI.
- Composites of carbon materials with metal nanoparticles increased their capacitive and salt removal performance [218,219]. Doping biobased carbon materials with metal nanoparticles such as ZnO, MoS_2, and TiO_2 were not tested yet; therefore, further investigation on this topic is recommended.
- MXene is a two-dimensional material that exhibited high performance in CDI applications [220,221], and its composite with carbon improved its performance [222,223]. Preparing MXene composite with bio-based carbon materials with and without doping with heteroatoms is expected to improve the performance of the CDI.
- Novel CDI cell structures, such as membrane CDI and flow-electrode CDI, were not tested using bio-based carbon electrodes. This investigation may result in an enhancement in the cells' performance and a reduction of the system's capital cost.

8. Conclusions

This work reviews the progress in applying bio-based carbon electrodes in the CDI systems. The different fabrication processes of bio-based electrodes of the CDI and their implementation for water desalination and wastewater treatment are summarized. It was found that most of the studies focused on plant-based wastes, and among the different electrodes, those included a heteroatom doping or metal nanoparticles showed the highest performance. Regarding the application of the bio-based carbon CDI electrods in wastewater treatment, the research focused on heavy metal ion removal (focusing on chromium). Bio-based carbon electrodes were compared to conventional carbon electrodes in terms of resource availability, ease of manufacture, cost, material specification, and CDI performance. The bio-based electrodes demonstrated better features in terms of availability, price, and fabrication, while they show a comparable performance compared to conventional carbon-based electrodes.

Declaration of Competing Interest

The authors declare that they have no known competing financial interests or personal relationships that could have appeared to influence the work reported in this paper.

Acknowledgement

This work was supported by the University of Sharjah, Project No. 19020406129.

References

[1] Abdelkareem MA, El Haj Assad M, Sayed ET, Soudan B. Recent progress in the use of renewable energy sources to power water desalination plants. Desalination 2018;435:97–113.
[2] Wilberforce T, Sayed ET, Abdelkareem MA, Elsaid K, Olabi AG. Value added products from wastewater using bioelectrochemical systems: current trends and perspectives. J Water Process Eng 2020:101737.
[3] Huang B-C, Lu Y, Li W-W. Exploiting the energy potential of municipal wastewater in China by incorporating tailored anaerobic treatment processes. Renew Energy 2020;158:534–40.
[4] Birjandi N, Younesi H, Ghoreyshi AA, Rahimnejad M. Enhanced medicinal herbs wastewater treatment in continuous flow bio-electro-Fenton operations along with power generation. Renew Energy 2020;155:1079–90.
[5] Miyawaki B, Mariano AB, Vargas JVC, Balmant W, Defrancheschi AC, Corrêa DO, et al. Microalgae derived biomass and bioenergy production enhancement through biogas purification and wastewater treatment. Renew Energy 2021;163:1153–65.
[6] Muhammad Anwar SNB, Alvarado V, Hsu S-C. A socio-eco-efficiency analysis of water and wastewater treatment processes for refugee communities in Jordan. Resour Conserv Recycl 2021;164:105196.
[7] Wilberforce T, Olabi AG, Sayed ET, Elsaid K, Abdelkareem MA. Progress in carbon capture technologies. Sci Total Environ 2020;143203.
[8] Obaid M, Abdelkareem MA, Kook S, Kim H-Y, Hilal N, Ghaffour N, et al. Breakthroughs in the fabrication of electrospun-nanofiber-supported thin film composite/nanocomposite membranes for the forward osmosis process: a review. Crit Rev Environ Sci Technol 2020;50:1727–95.
[9] Sayed ET, Al Radi M, Ahmad A, Abdelkareem MA, Alawadhi H, Atieh MA, et al. Faradic capacitive deionization (FCDI) for desalination and ion removal from wastewater. Chemosphere 2021;275:130001.
[10] Al Radi M, Sayed ET, Alawadhi H, Abdelkareem MA. Progress in energy recovery and graphene usage in capacitive deionization. Crit Rev Environ Sci Technol 2022;52:3080–136.
[11] Elsaid K, Elkamel A, Sayed ET, Wilberforce T, Abdelkareem MA, Olabi A-G. Carbon-Based Nanomaterial for Emerging Desalination Technologies: Electrodialysis and Capacitive Deionization. In: Olabi A-G, editor. Encyclopedia of Smart Materials. Oxford: Elsevier; 2022. p. 411–20.
[12] Xu H, Ji X, Wang L, Huang J, Han J, Wang Y. Performance study on a small-scale photovoltaic electrodialysis system for desalination. Renew Energy 2020;154:1008–13.
[13] AlMadani HMN. Water desalination by solar powered electrodialysis process. Renew Energy 2003;28:1915–24.
[14] Hansima M, Makehelwala M, Jinadasa K, Wei Y, Nanayakkara K, Herath AC, et al. Fouling of ion exchange membranes used in the electrodialysis reversal advanced water treatment: a review. Chemosphere 2020;127951.
[15] Sayed ET, Shehata N, Abdelkareem MA, Atieh MA. Recent progress in environmentally friendly bio-electrochemical devices for simultaneous water desalination and wastewater treatment. Sci Total Environ 2020;748:141046.
[16] Kokabian B, Ghimire U, Gude VG. Water deionization with renewable energy production in microalgae - microbial desalination process. Renew Energy 2018;122:354–61.
[17] Elsaid K, Sayed ET, Abdelkareem MA, Mahmoud MS, Ramadan M, Olabi AG. Environmental impact of emerging desalination technologies: a preliminary evaluation. J Environ Chem Eng 2020;8:104099.
[18] Ali A, Quist-Jensen CA, Jørgensen MK, Siekierka A, Christensen ML, Bryjak M, et al. A review of membrane crystallization, forward osmosis and membrane capacitive deionization for liquid mining. Resour Conserv Recycl 2020:105273.
[19] Cheng Y, Hao Z, Hao C, Deng Y, Li X, Li K, et al. A review of modification of carbon electrode material in capacitive deionization. RSC Adv 2019;9:24401–19.
[20] Wang L, Dykstra J, Lin S. Energy efficiency of capacitive deionization. Environ Sci Technol 2019;53:3366–78.
[21] Elisadiki J, Kibona TE, Machunda RL, Saleem MW, Kim W-S, Jande YAC. Biomass-based carbon electrode materials for capacitive deionization: a review. Biomass Convers Biorefin 2020;10:1327–56.
[22] Rabaia MKH, Abdelkareem MA, Sayed ET, Elsaid K, Chae K-J, Wilberforce T, et al. Environmental impacts of solar energy systems: a review. Sci Total Environ 2021;754:141989.
[23] Dykstra JE. Desalination with porous electrodes: mechanisms of ion transport and adsorption. Wageningen University; 2018.
[24] Yasin AS, Obaid M, Mohamed IM, Yousef A, Barakat NA. ZrO 2 nanofibers/activated carbon composite as a novel and effective electrode material for the enhancement of capacitive deionization performance. RSC Adv 2017;7:4616–26.
[25] Hawks SA, Ramachandran A, Porada S, Campbell PG, Suss ME, Biesheuvel P, et al. Performance metrics for the objective assessment of capacitive deionization systems. Water Res 2019;152:126–37.
[26] D.V. Fix, Capacitive Deionization of Seawater, 1995.
[27] Agartan L, Hayes-Oberst B, Byles BW, Akuzum B, Pomerantseva E, Kumbur EC. Influence of operating conditions and cathode parameters on desalination performance of hybrid CDI systems. Desalination 2019;452:1–8.

[28] Srimuk P, Zeiger M, Jäckel N, Tolosa A, Krüner B, Fleischmann S, et al. Enhanced performance stability of carbon/titania hybrid electrodes during capacitive deionization of oxygen saturated saline water. Electrochim Acta 2017;224:314–28.
[29] Sufiani O, Elisadiki J, Machunda RL, Jande YA. Modification strategies to enhance electrosorption performance of activated carbon electrodes for capacitive deionization applications. J Electroanal Chem 2019;848: 113328.
[30] Moustafa HM, Obaid M, Nassar MM, Abdelkareem MA, Mahmoud MS. Titanium dioxide-decorated rGO as an effective electrode for ultrahigh-performance capacitive deionization. Sep Purif Technol 2020;235: 116178.
[31] Moustafa HM, Nassar MM, Abdelkareem MA, Mahmoud MS, Obaid M. Synthesis and characterization of Co and Titania nanoparticle -intercalated rGO as a high capacitance electrode for CDI. J Environ Chem Eng 2019;7:103441.
[32] Moustafa HM, Nassar MM, Abdelkareem MA, Mahmoud MS, Obaid M. Synthesis of single and bimetallic oxide-doped rGO as a possible electrode for capacitive deionization. J Appl Electrochem 2020;50:745–55.
[33] Liu X, Shanbhag S, Natesakhawat S, Whitacre JF, Mauter MS. Performance loss of activated carbon electrodes in capacitive deionization: mechanisms and material property predictors. Environ Sci Technol 2020;54:15516–26.
[34] Xu X, Allah AE, Wang C, Tan H, Farghali AA, Khedr MH, et al. Capacitive deionization using nitrogen-doped mesostructured carbons for highly efficient brackish water desalination. Chem Eng J 2019;362:887–96.
[35] Bi Z, Kong Q, Cao Y, Sun G, Su F, Wei X, et al. Biomass-derived porous carbon materials with different dimensions for supercapacitor electrodes: a review. J Mater Chem A 2019;7:16028–45.
[36] Yang H, Ye S, Zhou J, Liang T. Biomass-derived porous carbon materials for supercapacitor. Front Chem 2019;7:274.
[37] Mehta S, Jha S, Liang H. Lignocellulose materials for supercapacitor and battery electrodes: A review. Renew Sustain Energy Rev 2020;134:110345.
[38] Hoffmann V, Jung D, Alhnidi MJ, Mackle L, Kruse A. Bio-based carbon materials from potato waste as electrode materials in supercapacitors. Energies 2020;13:2406.
[39] Kaur P, Verma G, Sekhon S. Biomass derived hierarchical porous carbon materials as oxygen reduction reaction electrocatalysts in fuel cells. Prog Mater Sci 2019;102:1–71.
[40] Li X, Guan BY, Gao S, Lou XWD. A general dual-templating approach to biomass-derived hierarchically porous heteroatom-doped carbon materials for enhanced electrocatalytic oxygen reduction. Energy Environ Sci 2019;12:648–55.
[41] Abdelkareem MA, Sayed ET, Mohamed HO, Obaid M, Rezk H, Chae K-J. Nonprecious anodic catalysts for low-molecular-hydrocarbon fuel cells: Theoretical consideration and current progress. Prog Energy Combust Sci 2020;77:100805.
[42] Peera SG, Maiyalagan T, Liu C, Ashmath S, Lee TG, Jiang Z, et al. A review on carbon and non-precious metal based cathode catalysts in microbial fuel cells. Int J Hydrogen Energy 2020.
[43] Lv Y, Li Y, Han C, Chen J, He Z, Zhu J, et al. Application of porous biomass carbon materials in vanadium redox flow battery. J Colloid Interface Sci 2020;566:434–43.
[44] Liu P, Wang Y, Liu J. Biomass-derived porous carbon materials for advanced lithium sulfur batteries. J Energy Chem 2019;34:171–85.
[45] Elisadiki J, Kibona TE, Machunda RL, Saleem MW, Kim W-S, Jande YAC. Biomass-based carbon electrode materials for capacitive deionization: a review. Biomass Convers Biorefin 2019.
[46] Zhao C, Liu G, Sun N, Zhang X, Wang G, Zhang Y, et al. Biomass-derived N-doped porous carbon as electrode materials for Zn-air battery powered capacitive deionization. Chem Eng J 2018;334:1270–80.
[47] Chaleawlert-umpon S, Pimpha N. Sustainable lignin-derived hierarchically porous carbon for capacitive deionization applications. New J Chem 2020;44:12058–67.
[48] Du Z, Tian W, Qiao K, Zhao J, Wang L, Xie W, et al. Improved chlorine and chromium ion removal from leather processing wastewater by biocharcoal-based capacitive deionization. Sep Purif Technol 2020;233:116024.
[49] Maniscalco M, Corrado C, Volpe R, Messineo A. Evaluation of the optimal activation parameters for almond shell bio-char production for capacitive deionization. Bioresource Technol Rep 2020:100435.
[50] Tang K, Hong TZX, You L, Zhou K. Carbon–metal compound composite electrodes for capacitive deionization: synthesis, development and applications. J Mater Chem A 2019;7:26693–743.
[51] Elisadiki J, King'ondu CK. Performance of ion intercalation materials in capacitive deionization/electrochemical deionization: a review. J Electroanal Chem 2020;114588.
[52] Elisadiki J, Kibona TE, Machunda RL, Saleem MW, Kim W-S, Jande YA. Biomass-based carbon electrode materials for capacitive deionization: a review. Biomass Convers Biorefin 2019:1–30.
[53] Liu Z, Wang Z, Tang S, Liu Z. Fabrication, characterization and sorption properties of activated biochar from livestock manure via three different approaches. Resour Conserv Recycl 2020:105254.
[54] Elkhalifa S, Al-Ansari T, Mackey HR, McKay G. Food waste to biochars through pyrolysis: a review. Resour Conserv Recycl 2019;144:310–20.
[55] Rezma S, Assaker IB, Chtourou R, Hafiane A, Deleuze H. Microporous activated carbon electrode derived from date stone without use of binder for capacitive deionization application. Mater Res Bull 2019;111:222–9.
[56] Vafakhah S, Beiramzadeh Z, Saeedikhani M, Yang HY. A review on free-standing electrodes for energy-effective desalination: recent advances and perspectives in capacitive deionization. Desalination 2020;493:114662.
[57] Zhao X, Wei H, Zhao H, Wang Y, Tang N. Electrode materials for capacitive deionization: a review. J Electroanal Chem 2020;114416.
[58] Kim N, Lee J, Kim S, Hong SP, Lee C, Yoon J, et al. Short review of multichannel membrane capacitive deionization: principle, current status, and future prospect. Appl Sci 2020;10:683.
[59] Maheshwari K, Agrawal M. Advances in capacitive deionization as an effective technique for reverse osmosis reject stream treatment. J Environ Chem Eng 2020:104413.
[60] Ntakirutimana S, Tan W, Anderson MA, Wang Y. Review—activated carbon electrode design: engineering tradeoff with respect to capacitive deionization performance. J Electrochem Soc 2020.
[61] Saidur R, Abdelaziz E, Demirbas A, Hossain M, Mekhilef S. A review on biomass as a fuel for boilers. Renew Sustain Energy Rev 2011;15:2262–89.
[62] Wang J, Nie P, Ding B, Dong S, Hao X, Dou H, et al. Biomass derived carbon for energy storage devices. J Mater Chem A 2017;5:2411–28.
[63] Thomas P, Lai CW, Johan MRB. Recent developments in biomass-derived carbon as a potential sustainable material for super-capacitor-based energy storage and environmental applications. J Anal Appl Pyrol 2019;140:54–85.
[64] Oliver-Tomas B, Hitzl M, Owsianiak M, Renz M. Evaluation of hydrothermal carbonization in urban mining for the recovery of phosphorus from the organic fraction of municipal solid waste. Resour Conserv Recycl 2019;147:111–8.
[65] Shen Y. A review on hydrothermal carbonization of biomass and plastic wastes to energy products. Biomass Bioenergy 2020;134:105479.
[66] Wang T, Zhai Y, Zhu Y, Li C, Zeng G. A review of the hydrothermal carbonization of biomass waste for hydrochar formation: process conditions, fundamentals, and physicochemical properties. Renew Sustain Energy Rev 2018;90:223–47.
[67] Kambo HS, Dutta A. A comparative review of biochar and hydrochar in terms of production, physico-chemical properties and applications. Renew Sustain Energy Rev 2015;45:359–78.
[68] Zhao P, Shen Y, Ge S, Chen Z, Yoshikawa K. Clean solid biofuel production from high moisture content waste biomass employing hydrothermal treatment. Appl Energy 2014;131:345–67.
[69] Tian J, Liu Z, Li Z, Wang W, Zhang H. Hierarchical S-doped porous carbon derived from by-product lignin for high-performance supercapacitors. RSC Adv 2017;7:12089–97.
[70] M.-M. Titirici, A. Funke, A. Kruse, Hydrothermal carbonization of biomass, in: Recent advances in Thermo-chemical conversion of biomass, Elsevier, 2015, pp. 325-352.
[71] Hossain R, Sahajwalla V. Microrecycling of waste flexible printed circuit boards for in-situ generation of O- and N-doped activated carbon with outstanding supercapacitance performance. Resour Conserv Recycl 2020:105221.
[72] Bazan-Wozniak A, Nowicki P, Pietrzak R. Production of new activated bio-carbons by chemical activation of residue left after supercritical extraction of hops. Environ Res 2018;161:456–63.
[73] Abioye AM, Ani FN. Recent development in the production of activated carbon electrodes from agricultural waste biomass for supercapacitors: a review. Renew Sustain Energy Rev 2015;52:1282–93.
[74] Huang Y, Liu Z, Zhao G. Reaction process for ZnCl 2 activation of phenol liquefied wood fibers. RSC Adv 2016;6:78909–17.
[75] Zhai Y, Dou Y, Zhao D, Fulvio PF, Mayes RT, Dai S. Carbon materials for chemical capacitive energy storage. Adv Mater 2011;23:4828–50.
[76] Alfredy T. Removal of heavy metals from water by capacitive deionization electrode materials derived from chicken feathers, in. NM-AIST 2019.
[77] Liu X. Ionothermal synthesis of carbon nanostructures: playing with carbon chemistry in inorganic salt melt. Nano Adv 2016;1:90.
[78] Fechler N, Wohlgemuth S-A, Jäker P, Antonietti M. Salt and sugar: direct synthesis of high surface area carbon materials at low temperatures via hydrothermal carbonization of glucose under hypersaline conditions. J Mater Chem A 2013;1:9418–21.
[79] Li G-X, Hou P-X, Zhao S-Y, Liu C, Cheng H-M. A flexible cotton-derived carbon sponge for high-performance capacitive deionization. Carbon 2016;101:1–8.
[80] Tang Y-H, Liu S-H, Tsang DC. Microwave-assisted production of CO2-activated biochar from sugarcane bagasse for electrochemical desalination. J Hazard Mater 2020;383:121192.
[81] Lado JJ, Zornitta RL, Calvi FA, Martins M, Anderson MA, Nogueira FG, et al. Enhanced capacitive deionization desalination provided by chemical activation of sugar cane bagasse fly ash electrodes. J Anal Appl Pyrol 2017;126:143–53.
[82] Lado JJ, Zornitta RL, Vazquez Rodriguez I, Malverdi Barcelos K, Ruotolo LA. Sugarcane biowaste-derived biochars as capacitive deionization electrodes for brackish water desalination and water-softening applications. ACS Sustain Chem Eng 2019;7:18992–9004.
[83] Pode R. Potential applications of rice husk ash waste from rice husk biomass power plant. Renew Sustain Energy Rev 2016;53:1468–85.
[84] Zhang J, Jin J, Wang M, Naidu R, Liu Y, Man YB, et al. Co-pyrolysis of sewage sludge and rice husk/ bamboo sawdust for biochar with high aromaticity and low metal mobility. Environ Res 2020;191:110034.
[85] Cuong DV, Wu P-C, Liu N-L, Hou C-H. Hierarchical porous carbon derived from activated biochar as an eco-friendly electrode for the electrosorption of inorganic ions. Sep Purif Technol 2020;116813.

[86] Silva AP, Argondizo A, Juchen PT, Ruotolo LA. Ultrafast capacitive deionization using rice husk activated carbon electrodes. Sep Purif Technol 2021;271:118872.
[87] V. Pavlenko, Z. Supiyeva, Application of Carbons Produced from Rice Husk in the Process of Capacitive Deionization, Eurasian Chemico-Technological Journal, 22 (2020) 277-284-277-284.
[88] Kim J, Yi Y, Peck D-H, Yoon S-H, Jung D-H, Park HS. Controlling hierarchical porous structures of rice-husk-derived carbons for improved capacitive deionization performance. Environ Sci NANO 2019;6:916–24.
[89] Yan J, Zhang H, Xie Z, Liu J. Preparation of the Lentinus edodes-based porous biomass carbon by hydrothermal method for capacitive desalination, in. AIP Conference Proceedings, AIP Publishing LLC 2017:020218.
[90] Liu K, Chen B, Feng A, Wu J, Hu X, Zhou J, et al. Bio-composite nanoarchitectonics for graphene tofu as useful source material for capacitive deionization. Desalination 2022;526:115461.
[91] Zhuang R, Xu L, Da Li NM, Chen J, Yu Y, Song H, et al. Acidified bamboo-derived activated carbon/manganese dioxide composite as a high-performance electrode material for capacitive deionization. Int J Electrochem Sci 2020;15:3104–18.
[92] Govindan B, Alhseinat E, Darawsheh IF, Ismail I, Polychronopoulou K, Abi Jaoude M, et al. Activated carbon derived from phoenix dactylifera (Palm Tree) and decorated with MnO2 nanoparticles for enhanced hybrid capacitive deionization electrodes. ChemistrySelect 2020;5:3248–56.
[93] Kyaw HH, Al-Mashaikhi SM, Myint MTZ, Al-Harthi S, El-Shafey E-S-I, Al-Abri M. Activated carbon derived from the date palm leaflets as multifunctional electrodes in capacitive deionization system. Chem Eng Process-Process Intensification 2021;161:108311.
[94] Sayed DM, El-Deab MS, Allam NK. Multi-walled vanadium oxide nanotubes modified 3D microporous bioderived carbon as novel electrodes for hybrid capacitive deionization. Sep Purif Technol 2021;266:118597.
[95] Chen P-A, Cheng H-C, Wang HP. Activated carbon recycled from bitter-tea and palm shell wastes for capacitive desalination of salt water. J Cleaner Prod 2018;174:927–32.
[96] Hai A, Bharath G, Babu KR, Taher H, Naushad M, Banat F. Date seeds biomass-derived activated carbon for efficient removal of NaCl from saline solution. Process Saf Environ Prot 2019;129:103–11.
[97] Ye W, Tang J, Wang Y, Cai X, Liu H, Lin J, et al. Hierarchically structured carbon materials derived from lotus leaves as efficient electrocatalyst for microbial energy harvesting. Sci Total Environ 2019;666:865–74.
[98] Liu G, Qiu L, Deng H, Wang J, Yao L, Deng L. Ultrahigh surface area carbon nanosheets derived from lotus leaf with super capacities for capacitive deionization and dye adsorption. Appl Surf Sci 2020;146485.
[99] Ma X, Wu Q, Wang WA, Lu S, Xiang Y, Aurbach D. Mass-producible polyhedral macrotube carbon arrays with multi-hole cross-section profiles: superb 3D tertiary porous electrode materials for supercapacitors and capacitive deionization cells. J Mater Chem A 2020;8:16312–22.
[100] Xing W, Zhang M, Liang J, Tang W, Li P, Luo Y, et al. Facile synthesis of pinecone biomass-derived phosphorus-doping porous carbon electrodes for efficient electrochemical salt removal. Sep Purif Technol 2020;251:117357.
[101] Samaraweera H, Pittman CU, Thirumalai RVKG, Hassan EB, Perez F, Mlsna T. Characterization of graphene/pine wood biochar hybrids: Potential to remove aqueous Cu2+. Environ Res 2021;192:110283.
[102] Liu Q, Li X, Wu Y, Qing M, Tan G, Xiao D. Pine pollen derived porous carbon with efficient capacitive deionization performance. Electrochim Acta 2019;298:360–71.
[103] Pan B, Wang Y, Li H, Yi W, Pan Y. Preparation and electrosorption desalination performance of peanut shell-based activated carbon and MoS2. Int J Electrochem Sci 2020;15:1861–80.
[104] Feng C, Chen Y-A, Yu C-P, Hou C-H. Highly porous activated carbon with multi-channeled structure derived from loofa sponge as a capacitive electrode material for the deionization of brackish water. Chemosphere 2018;208:285–93.
[105] Sriramulu D, Vafakhah S, Yang HY. Activated Luffa derived biowaste carbon for enhanced desalination performance in brackish water. RSC Adv 2019;9:14884–92.
[106] Pham TN, Nguyen TH, Le VH, Nguyen TT, Nguyen TDK, Tran TN, et al. Coconut shell-derived activated carbon and carbon nanotubes composite: a promising candidate for capacitive deionization electrode. Synth Met 2020;265:116415.
[107] Adorna Jr J, Borines M, Doong R-A. Coconut shell derived activated biochar–manganese dioxide nanocomposites for high performance capacitive deionization. Desalination 2020;492:114602.
[108] Nguyen TT, Pham TN, Tran TN, Ho TTN, Dai Nguyen T, Nguyen TTT, et al. Enhanced capacitive deionization performance of activated carbon derived from coconut shell electrodes with low content carbon nanotubes–graphene synergistic hybrid additive. Mater Lett 2021;292:129652.
[109] Rangaraj VM, Edathil AA, Kannangara YY, Song J-K, Haija MA, Banat F. Tamarind shell derived N-doped carbon for capacitive deionization (CDI) studies. J Electroanal Chem 2019;848:113307.
[110] Elisadiki J, Jande YAC, Machunda RL, Kibona TE. Porous carbon derived from Artocarpus heterophyllus peels for capacitive deionization electrodes. Carbon 2019;147:582–93.
[111] Xie Z, Shang X, Yan J, Hussain T, Nie P, Liu J. Biomass-derived porous carbon anode for high-performance capacitive deionization. Electrochim Acta 2018;290:666–75.
[112] Rambabu K, Bharath G, Hai A, Luo S, Liao K, Haijaa MA, et al. Development of watermelon rind derived activated carbon/manganese ferrite nanocomposite for cleaner desalination by capacitive deionization. J Cleaner Prod 2020;122626.
[113] Zhang R, Gu X, Liu Y, Hua D, Shao M, Gu Z, et al. Hydrophilic nano-porous carbon derived from egg whites for highly efficient capacitive deionization. Appl Surf Sci 2020;512:145740.
[114] Liu Y, Zhang X, Gu X, Wu N, Zhang R, Shen Y, et al. One-step turning leather wastes into heteroatom doped carbon aerogel for performance enhanced capacitive deionization. Microporous Mesoporous Mater 2020;110303.
[115] Santos VP, Marques NS, Maia PC, Lima MABd, Franco LdO, Campos-Takaki GMd. Seafood waste as attractive source of chitin and chitosan production and their applications, Int. J. Mol. Sci. 21 (2020) 4290.
[116] Wu Q, Liang D, Ma X, Lu S, Xiang Y. Chitosan-based activated carbon as economic and efficient sustainable material for capacitive deionization of low salinity water. RSC Adv 2019;9:26676–84.
[117] Weng J, Wang S, Wang G, Zhang P, Lu B, Wang H, et al. Carbon electrode with cross-linked and charged chitosan binder for enhanced capacitive deionization performance. Desalination 2021;505:114979.
[118] Szabó L, Xu X, Uto K, Henzie J, Yamauchi Y, Ichinose I, et al. Tailoring the structure of chitosan-based porous carbon nanofiber architectures toward efficient capacitive charge storage and capacitive deionization. ACS Appl Mater Interfaces 2022.
[119] Xie Z, Shang X, Yang J, Hu B, Nie P, Jiang W, et al. 3D interconnected boron- and nitrogen-codoped carbon nanosheets decorated with manganese oxides for high-performance capacitive deionization. Carbon 2020;158:184–92.
[120] Geyer R, Jambeck JR, Law KL. Production, use, and fate of all plastics ever made. Sci Adv 2017;3:e1700782.
[121] Deka N, Barman J, Kasthuri S, Nutalapati V, Dutta GK. Transforming waste polystyrene foam into N-doped porous carbon for capacitive energy storage and deionization applications. Appl Surf Sci 2020;511:145576.
[122] Porada S, Schipper F, Aslan M, Antonietti M, Presser V, Fellinger T-P. Capacitive deionization using biomass-based microporous salt-templated heteroatom-doped carbons; 2015.
[123] Mohamed SK, Abuelhamd M, Allam NK, Shahat A, Ramadan M, Hassan HM. Eco-friendly facile synthesis of glucose–derived microporous carbon spheres electrodes with enhanced performance for water capacitive deionization. Desalination 2020;477:114278.
[124] Yang T, Li W, Ogunbiyi AT, An S. Efficient catalytic conversion of corn stover to furfural and 5-hydromethylfurfural using glucosamine hydrochloride derived carbon solid acid in γ-valerolactone. Ind Crops Product 161 113173.
[125] Kim HS, Park YH, Kim S, Choi Y-E. Application of a polyethylenimine-modified polyacrylonitrile-biomass waste composite fiber sorbent for the removal of a harmful cyanobacterial species from an aqueous solution. Environ Res 2020;190:109997.
[126] Zare EN, Motahari A, Sillanpää M. Nanoadsorbents based on conducting polymer nanocomposites with main focus on polyaniline and its derivatives for removal of heavy metal ions/dyes: a review. Environ Res 2018;162:173–95.
[127] Wang Z, Huang L, Wang Y, Chen X, Ren H. Activation of peroxymonosulfate using metal-free in situ N-doped carbonized polypyrrole: a non-radical process. Environ Res 2021;193:110537.
[128] Zornitta RL, García-Mateos FJ, Lado JJ, Rodríguez-Mirasol J, Cordero T, Hammer P, et al. High-performance activated carbon from polyaniline for capacitive deionization. Carbon 2017;123:318–33.
[129] Krüner B, Srimuk P, Fleischmann S, Zeiger M, Schreiber A, Aslan M, et al. Hydrogen-treated, sub-micrometer carbon beads for fast capacitive deionization with high performance stability. Carbon 2017;117:46–54.
[130] Qian W, Sun F, Xu Y, Qiu L, Liu C, Wang S, et al. Human hair-derived carbon flakes for electrochemical supercapacitors. Energy Environ Sci 2014;7:379–86.
[131] Nwankwo I, Nwaiwu N, Nwabanne J. Production and characterization of activated carbon from animal bone. Am J Eng Res (AJER) E-ISSN 2018:2320–10847.
[132] Xing W, Zhang M, Liang J, Tang W, Li P, Luo Y, et al. Facile synthesis of pinecone biomass-derived phosphorus-doping porous carbon electrodes for efficient electrochemical salt removal. Sep Purif Technol 2020;117357.
[133] Wang S, Feng J, Meng Q, Cao B, Tian G. Study on boron and nitrogen co-doped graphene xerogel for high-performance electrosorption application. J Solid State Electrochem 2019;23:2377–90.
[134] Jia B, Zou L. Wettability and its influence on graphene nansoheets as electrode material for capacitive deionization. Chem Phys Lett 2012;548:23–8.
[135] Han D-C, Zhang C-M, Guan J, Gai L-H, Yue R-Y, Liu L-N, et al. High-performance capacitive deionization using nitrogen and phosphorus-doped three-dimensional graphene with tunable pore size. Electrochim Acta 2020;135639.
[136] Yousef A, Al-Enizi AM, Mohamed IM, El-Halwany M, Ubaidullah M, Brooks RM. Synthesis and characterization of CeO2/rGO nanoflakes as electrode material for capacitive deionization technology. Ceram Int 2020.
[137] Peng W, Wang W, Han G, Huang Y, Zhang Y. Fabrication of 3D flower-like MoS2/graphene composite as high-performance electrode for capacitive deionization. Desalination 2020;473:114191.

[138] Arora N, Banat F, Bharath G, Alhseinat E. Capacitive deionization of NaCl from saline solution using graphene/CNTs/ZnO NPs based electrodes. J Phys D Appl Phys 2019;52:455304.
[139] Lado JJ, Zornitta RL, Calvi FA, Tejedor-Tejedor MI, Anderson MA, Ruotolo LA. Study of sugar cane bagasse fly ash as electrode material for capacitive deionization. J Anal Appl Pyrol 2016;120:389–98.
[140] Islam D, Hasan MS. A novel approach for purifying contaminated drinking water using carbon aerogel electrodes synthesized from thermoplastic waste.
[141] Bartels CR, Wilf M, Andes K, Iong J. Design considerations for wastewater treatment by reverse osmosis. Water Sci Technol 2005;51:473–82.
[142] Sayed ET, Nakagawa N. Critical issues in the performance of yeast based microbial fuel cell. J Chem Technol Biotechnol 2018;93:1588–94.
[143] Shon H, Phuntsho S, Chaudhary D, Vigneswaran S, Cho J. Nanofiltration for water and wastewater treatment-a mini review. Drinking Water Engineering and Science 2013.
[144] Abdallah M, Feroz S, Alani S, Sayed ET, Shanableh A. Continuous and scalable applications of microbial fuel cells: a critical review. Rev. Enviro. Sci. Bio/Technology 2019;18:543–78.
[145] Sayed ET, Alawadhi H, Elsaid K, Olabi AG, Adel Almakrani M, Bin Tamim ST, et al. A carbon-cloth anode electroplated with iron nanostructure for microbial fuel cell operated with real wastewater. Sustainability 2020;12:6538.
[146] Mohamed HO, Obaid M, Sayed ET, Abdelkareem MA, Park M, Liu Y, et al. Graphite sheets as high-performance low-cost anodes for microbial fuel cells using real food wastewater. Chem Eng Technol 2017;40:2243–50.
[147] Sayed ET, Alawadhi H, Olabi AG, Jamal A, Almahdi MS, Khalid J, et al. Electrophoretic deposition of graphene oxide on carbon brush as bioanode for microbial fuel cell operated with real wastewater. Int J Hydrogen Energy 2021;46:5975–83.
[148] Sayed ET, Abdelkareem MA, Alawadhi H, Elsaid K, Wilberforce T, Olabi AG. Graphitic carbon nitride/carbon brush composite as a novel anode for yeast-based microbial fuel cells. Energy 2021;221:119849.
[149] Sud D, Mahajan G, Kaur M. Agricultural waste material as potential adsorbent for sequestering heavy metal ions from aqueous solutions – a review. Bioresour Technol 2008;99:6017–27.
[150] Rambabu K, Bharath G, Banat F, Show PL. Biosorption performance of date palm empty fruit bunch wastes for toxic hexavalent chromium removal. Environ Res 2020;187:109694.
[151] Bharath G, Rambabu K, Banat F, Hai A, Arangadi AF, Ponpandian N. Enhanced electrochemical performances of peanut shell derived activated carbon and its Fe3O4 nanocomposites for capacitive deionization of Cr (VI) ions. Sci Total Environ 2019;691:713–26.
[152] Gaikwad MS, Balomajumder C. Tea waste biomass activated carbon electrode for simultaneous removal of Cr (VI) and fluoride by capacitive deionization. Chemosphere 2017;184:1141–9.
[153] Gaikwad MS, Balomajumder C, Tiwari AK. Acid treated RHWBAC electrode performance for Cr (VI) removal by capacitive deionization and CFD analysis study. Chemosphere 2020;126781.
[154] Zhang X, Wang B, Yu J, Wu X, Zang Y, Gao H, et al. Three-dimensional honeycomb-like porous carbon derived from corncob for the removal of heavy metals from water by capacitive deionization. RSC Adv 2018;8:1159–67.
[155] Jss A. Biocomposite based electrode for effective removal of Cr (VI) heavy metal via capacitive deionization. Chem Eng Commun 2020;207:775–89.
[156] Chang Y, Dang Q, Samo I, Li Y, Li X, Zhang G, et al. Electrochemical heavy metal removal from water using PVC waste-derived N, S co-doped carbon materials. RSC Adv 2020;10:4064–70.
[157] Wang H, Wang J, Xiang X, Zhou Y, Li Q, Tang A, et al. Preparation of PVDF/CdS/Bi2WO6/ZnO hybrid membrane with enhanced visible-light photocatalytic activity for degrading nitrite in water. Environ Res 2020;191:110036.
[158] Cheng H, Zhu Q, Wang A, Weng M, Xing Z. Composite of chitosan and bentonite cladding Fe–Al bimetal: Effective removal of nitrate and by-products from wastewater. Environ Res 2020;184:109336.
[159] Zhou R-Y, Yu J-X, Chi R-A. Selective removal of phosphate from aqueous solution by MIL-101(Fe)/bagasse composite prepared through bagasse size control. Environ Res 2020;188:109817.
[160] Li D, Ning X-A, Yuan Y, Hong Y, Zhang J. Ion-exchange polymers modified bacterial cellulose electrodes for the selective removal of nitrite ions from tail water of dyeing wastewater. J Environ Sci 2020;91:62–72.
[161] Lofrano G, Meriç S, Zengin GE, Orhon D. Chemical and biological treatment technologies for leather tannery chemicals and wastewaters: a review. Sci Total Environ 2013;461:265–81.
[162] Wang Q, Zhang Y, Jiang H, Meng C. In-situ grown manganese silicate from biomass-derived heteroatom-doped porous carbon for supercapacitors with high performance. J Colloid Interface Sci 2019;534:142–55.
[163] Wang Z, Tan Y, Yang Y, Zhao X, Liu Y, Niu L, et al. Pomelo peels-derived porous activated carbon microsheets dual-doped with nitrogen and phosphorus for high performance electrochemical capacitors. J Power Sources 2018;378:499–510.
[164] Zhang M, Jin X, Wang L, Sun M, Tang Y, Chen Y, et al. Improving biomass-derived carbon by activation with nitrogen and cobalt for supercapacitors and oxygen reduction reaction. Appl Surf Sci 2017;411:251–60.
[165] Yang S, Wang S, Liu X, Li L. Biomass derived interconnected hierarchical micro-meso-macro-porous carbon with ultrahigh capacitance for supercapacitors. Carbon 2019;147:540–9.
[166] Liu S, Zhao Y, Zhang B, Xia H, Zhou J, Xie W, et al. Nano-micro carbon spheres anchored on porous carbon derived from dual-biomass as high rate performance supercapacitor electrodes. J Power Sources 2018;381:116–26.
[167] Cai N, Cheng H, Jin H, Liu H, Zhang P, Wang M. Porous carbon derived from cashew nut husk biomass waste for high-performance supercapacitors. J Electroanal Chem 2020;861:113933.
[168] Pourhosseini S, Norouzi O, Naderi HR. Study of micro/macro ordered porous carbon with olive-shaped structure derived from Cladophora glomerata macroalgae as efficient working electrodes of supercapacitors. Biomass Bioenergy 2017;107:287–98.
[169] Pourhosseini S, Norouzi O, Salimi P, Naderi HR. Synthesis of a novel interconnected 3D pore network algal biochar constituting iron nanoparticles derived from a harmful marine biomass as high-performance asymmetric supercapacitor electrodes. ACS Sustain Chem Eng 2018;6:4746–58.
[170] Wang J, Zhang P, Liu L, Zhang Y, Yang J, Zeng Z, et al. Controllable synthesis of bifunctional porous carbon for efficient gas-mixture separation and high-performance supercapacitor. Chem Eng J 2018;348:57–66.
[171] Zhuo H, Hu Y, Tong X, Zhong L, Peng X, Sun R. Sustainable hierarchical porous carbon aerogel from cellulose for high-performance supercapacitor and CO2 capture. Ind Crops Prod 2016;87:229–35.
[172] Sevilla M, Ferrero GA, Fuertes AB. One-pot synthesis of biomass-based hierarchical porous carbons with a large porosity development. Chem Mater 2017;29:6900–7.
[173] Huang W, Zhang H, Huang Y, Wang W, Wei S. Hierarchical porous carbon obtained from animal bone and evaluation in electric double-layer capacitors. Carbon 2011;49:838–43.
[174] Sankar S, Ahmed ATA, Inamdar AI, Im H, Im YB, Lee Y, et al. Biomass-derived ultrathin mesoporous graphitic carbon nanoflakes as stable electrode material for high-performance supercapacitors. Mater Des 2019;169:107688.
[175] Yun YS, Cho SY, Shim J, Kim BH, Chang SJ, Baek SJ, et al. Microporous carbon nanoplates from regenerated silk proteins for supercapacitors. Adv Mater 2013;25:1993–8.
[176] Jin Z, Yan X, Yu Y, Zhao G. Sustainable activated carbon fibers from liquefied wood with controllable porosity for high-performance supercapacitors. J Mater Chem A 2014;2:11706–15.
[177] Mohammed AA, Chen C, Zhu Z. Low-cost, high-performance supercapacitor based on activated carbon electrode materials derived from baobab fruit shells. J Colloid Interface Sci 2019;538:308–19.
[178] Subramanian V, Luo C, Stephan AM, Nahm K, Thomas S, Wei B. Supercapacitors from activated carbon derived from banana fibers. J Phys Chem C 2007;111:7527–31.
[179] Mohammed AA, Chen C, Zhu Z. Green and high performance all-solid-state supercapacitors based on MnO2/Faidherbia albida fruit shell derived carbon sphere electrodes. J Power Sources 2019;417:1–13.
[180] Bhattacharjya D, Yu J-S. Activated carbon made from cow dung as electrode material for electrochemical double layer capacitor. J Power Sources 2014;262:224–31.
[181] Hou C-H, Liu N-L, Hsi H-C. Highly porous activated carbons from resource-recovered Leucaena leucocephala wood as capacitive deionization electrodes. Chemosphere 2015;141:71–9.
[182] Ahmed MA, Tewari S. Capacitive deionization: processes, materials and state of the technology. J Electroanal Chem 2018;813:178–92.
[183] Dias JM, Alvim-Ferraz MC, Almeida MF, Rivera-Utrilla J, Sánchez-Polo M. Waste materials for activated carbon preparation and its use in aqueous-phase treatment: a review. J Environ Manage 2007;85:833–46.
[184] Tamon H, Ishizaka H, Mikami M, Okazaki M. Porous structure of organic and carbon aerogels synthesized by sol-gel polycondensation of resorcinol with formaldehyde. Carbon 1997;35:791–6.
[185] Takeuchi K, Hayashi T, Kim Y, Fujisawa K, Endo M. The state-of-the-art science and applications of carbon nanotubes, Наносистемы: физика, химия, математика, 5 (2014).
[186] Liu H, Ning W, Cheng P, Zhang J, Wang Y, Zhang C. Evaluation of animal hairs-based activated carbon for sorption of norfloxacin and acetaminophen by comparing with cattail fiber-based activated carbon. J Anal Appl Pyrol 2013;101:156–65.
[187] Marsh H, Reinoso FR. Activated carbon. Elsevier; 2006.
[188] Chen Y, Zhu Y, Wang Z, Li Y, Wang L, Ding L, et al. Application studies of activated carbon derived from rice husks produced by chemical-thermal process—a review. Adv Colloid Interface Sci 2011;163:39–52.
[189] El-Deen AG, Barakat NA, Khalil KA, Kim HY. Hollow carbon nanofibers as an effective electrode for brackish water desalination using the capacitive deionization process. New J Chem 2014;38:198–205.
[190] Lu H, Zhao X. Biomass-derived carbon electrode materials for supercapacitors. Sustain Energy Fuels 2017;1:1265–81.
[191] Liu M, Xu M, Xue Y, Ni W, Huo S, Wu L, et al. Efficient capacitive deionization using natural basswood-derived, freestanding, hierarchically porous carbon electrodes. ACS Appl Mater Interfaces 2018;10:31260–70.
[192] Xu D, Tong Y, Yan T, Shi L, Zhang D. N, P-codoped meso-/microporous carbon derived from biomass materials via a dual-activation strategy as high-performance electrodes for deionization capacitors. ACS Sustain Chem Eng 2017;5:5810–9.
[193] Zhang J, Fang J, Han J, Yan T, Shi L, Zhang D. N, P, S co-doped hollow carbon polyhedra derived from MOF-based core–shell nanocomposites for capacitive deionization. J Mater Chem A 2018;6:15245–52.

[194] Aslan M, Zeiger M, Jäckel N, Grobelsek I, Weingarth D, Presser V. Improved capacitive deionization performance of mixed hydrophobic/hydrophilic activated carbon electrodes. J Phys: Condens Matter 2016;28:114003.
[195] Villar I, Roldan S, Ruiz V, Granda M, Blanco C, Menéndez R, et al. Capacitive deionization of NaCl solutions with modified activated carbon electrodes. Energy Fuels 2010;24:3329–33.
[196] Bonaccorso F, Colombo L, Yu G, Stoller M, Tozzini V, Ferrari AC, et al. Graphene, related two-dimensional crystals, and hybrid systems for energy conversion and storage. Science 2015;347.
[197] Peigney A, Laurent C, Flahaut E, Bacsa R, Rousset A. Specific surface area of carbon nanotubes and bundles of carbon nanotubes. Carbon 2001;39:507–14.
[198] Liu Y, Nie C, Liu X, Xu X, Sun Z, Pan L. Review on carbon-based composite materials for capacitive deionization. RSC Adv 2015;5:15205–25.
[199] Dreyer DR, Todd AD, Bielawski CW. Harnessing the chemistry of graphene oxide. Chem Soc Rev 2014;43:5288–301.
[200] Punetha VD, Rana S, Yoo HJ, Chaurasia A, McLeskey Jr JT, Ramasamy MS, et al. Functionalization of carbon nanomaterials for advanced polymer nanocomposites: a comparison study between CNT and graphene. Prog Polym Sci 2017;67:1–47.
[201] Thines R, Mubarak N, Nizamuddin S, Sahu J, Abdullah E, Ganesan P. Application potential of carbon nanomaterials in water and wastewater treatment: a review. J Taiwan Inst Chem Eng 2017;72:116–33.
[202] Zhao S, Yan T, Wang Z, Zhang J, Shi L, Zhang D. Removal of NaCl from saltwater solutions using micro/mesoporous carbon sheets derived from watermelon peel via deionization capacitors. RSC Adv 2017;7:4297–305.
[203] Wimalasiri Y, Zou L. Carbon nanotube/graphene composite for enhanced capacitive deionization performance. Carbon 2013;59:464–71.
[204] Wang L, Wang M, Huang Z-H, Cui T, Gui X, Kang F, et al. Capacitive deionization of NaCl solutions using carbon nanotube sponge electrodes. J Mater Chem 2011;21:18295–9.
[205] Kohli D, Singh R, Singh A, Bhartiya S, Singh M, Gupta P. Enhanced salt-adsorption capacity of ambient pressure dried carbon aerogel activated by CO2 for capacitive deionization application. Desalin Water Treat 2015;54:2825–31.
[206] Qian M, Xuan XY, Pan LK, Gong SQ. Porous carbon electrodes from activated wasted coffee grounds for capacitive deionization. Ionics 2019;25:3443–52.
[207] Wang G, Qian B, Dong Q, Yang J, Zhao Z, Qiu J. Highly mesoporous activated carbon electrode for capacitive deionization. Sep Purif Technol 2013;103:216–21.
[208] Dehkhoda AM, Ellis N, Gyenge E. Effect of activated biochar porous structure on the capacitive deionization of NaCl and ZnCl2 solutions. Microporous Mesoporous Mater 2016;224:217–28.
[209] Li J, Ji B, Jiang R, Zhang P, Chen N, Zhang G, et al. Hierarchical hole-enhanced 3D graphene assembly for highly efficient capacitive deionization. Carbon 2018;129:95–103.
[210] Zou L, Li L, Song H, Morris G. Using mesoporous carbon electrodes for brackish water desalination. Water Res 2008;42:2340–8.
[211] Farmer J. Method and apparatus for capacitive deionization, electrochemical purification, and regeneration of electrodes, in: Google Patents; 1995.
[212] Wang S, Wang D, Ji L, Gong Q, Zhu Y, Liang J. Equilibrium and kinetic studies on the removal of NaCl from aqueous solutions by electrosorption on carbon nanotube electrodes. Sep Purif Technol 2007;58:12–6.
[213] Liu Y, Pan L, Chen T, Xu X, Lu T, Sun Z, et al. Porous carbon spheres via microwave-assisted synthesis for capacitive deionization. Electrochim Acta 2015;151:489–96.
[214] Wang Z, Dou B, Zheng L, Zhang G, Liu Z, Hao Z. Effective desalination by capacitive deionization with functional graphene nanocomposite as novel electrode material. Desalination 2012;299:96–102.
[215] Liu Y, Cao L, Luo J, Peng Y, Ji Q, Dai J, et al. Biobased nitrogen- and oxygen-codoped carbon materials for high-performance supercapacitor. ACS Sustainable Chem Eng 2019;7:2763–73.
[216] Li P, Yang C, Wu C, Wei Y, Jiang B, Jin Y, et al. Bio-based carbon materials for high-performance supercapacitors. Nanomaterials 2022;12:2931.
[217] S. Parida, D.P. Dutta, Nanostructured Materials from Biobased Precursors for Renewable Energy Storage Applications, in: Biorenewable Nanocomposite Materials, Vol. 1: Electrocatalysts and Energy Storage, American Chemical Society, 2022, pp. 307-366.
[218] Han J, Yan T, Shen J, Shi L, Zhang J, Zhang D. Capacitive deionization of saline water by using MoS2–graphene hybrid electrodes with high volumetric adsorption capacity. Environ Sci Technol 2019;53:12668–76.
[219] Moustafa HM, Nassar MM, Abdelkareem MA, Mahmoud MS, Obaid M. Synthesis and characterization of Co and Titania nanoparticle-intercalated rGO as a high capacitance electrode for CDI. J Environ Chem Eng 2019;7:103441.
[220] Ma J, Cheng Y, Wang L, Dai X, Yu F. Free-standing Ti3C2Tx MXene film as binder-free electrode in capacitive deionization with an ultrahigh desalination capacity. Chem Eng J 2020;384:123329.
[221] Chen B, Feng A, Deng R, Liu K, Yu Y, Song L. MXene as a cation-selective cathode material for asymmetric capacitive deionization. ACS Appl Mater Interfaces 2020;12:13750–8.
[222] Torkamanzadeh M, Wang L, Zhang Y, Budak O, Srimuk P, Presser V. MXene/activated-carbon hybrid capacitive deionization for permselective ion removal at low and high salinity. ACS Appl Mater Interfaces 2020;12:26013–25.
[223] Zhang Y, Zhou J, Wang D, Cao R, Li J. Performance of MXene incorporated MOF-derived carbon electrode on deionization of Uranium (VI). Chem Eng J 2021;132702.

Dr. Enas Taha Sayed. Dr. Enas is associate professor at chemical engineering department, Minia university, Egypt. She got her PhD in bio-electrochemical systems from chemical and environmental engineering department, Gunma university, Gunma, Japan. Dr. Enas' research focuses on the fabrication of high conductive, high surface area, and biocompatible electrodes of the MFCs for simultaneous wastewater treatment and electricity generation. Also she is working on the development and application of graphene in wastewater treatment and water desalination. Dr Enas published around 100 manuscripts in ISI indexed journals Dr Enas successfully secured two national and internal grants with more than 600,000 USD. Dr Enas has already supervised several master and PhD students some of them already graduated and others not yet. Dr Enas is Editor in Scientific reports (Nature).

Prof. Abdul-Ghani Olabi. Prof Olabi is the Director of Sustainable Energy and Power Systems Research Centre at the University of Sharjah "UoS". Previously, he was Head of Department, Director of research institute, and many other academic and industrial position. He has supervised postgraduate research students (38 PhD) to successful completion. He has patented 2 innovative projects on PEM Fuel Call. He is the Subject Editor of the Elsevier Energy Journal, EiC of the Encyclopedia of Smart Materials (Elsevier), Editor of the Reference Module of Materials Science and Engineering (Elsevier), EiC of Renewable Energy section of Energies and board member of few other journals. Professor Olabi published more than 350 manuscripts in ISI indexed journals

Prof. Mohammad Ali Abdelkareem. Mohammad Abdelkareem got his PhD from Japan in 2008. Right now, he is professor in sustainable and renewable energy engineering department, university of Sharjah, UAE. He is working on the development of the different renewable energy resources and devices that can be used in wastewater treatment and water desalination. Moreover, He is working on the development of the electrodes for the different electrochemical energy conversion/storage devices, such as direct methanol fuel cells, direct urea fuel cells, microbial fuel cells, and supercapacitors. Professor Mohammad published more than 200 manuscripts in ISI indexed journals. He secured several research funds with more than 800,000 USD. He is editor in International journal of thermofluids and journal of carbon resources and conversion.